

Challenges and developments in wire arc additive manufacturing of steel: a review.

DEKIS, M., TAWFIK, M., EGIZA, M. and DEWIDAR, M.

2025

© 2025 Published by Elsevier B.V.

This is an open access article under the CC BY-NC-ND license (<http://creativecommons.org/licenses/by-nc-nd/4.0/>).



Review article

Challenges and developments in wire arc additive manufacturing of steel: A review

Mohamed Dekis^{a,*}, Mahmoud Tawfik^a, Mohamed Egiza^{a,b}, Montaser Dewidar^{a,c}

^a Department of Mechanical Engineering, Faculty of Engineering, Kafrelsheikh University, Kafrelsheikh 33516, Egypt

^b School of Engineering, Robert Gordon University, Garthdee Road, Aberdeen, AB10 7GJ, UK

^c Samannoud Technological University, Samannoud, Gharbia, Egypt

ARTICLE INFO

Keywords:

Defects
Mechanical properties
Microstructure
Steel
WAAM

ABSTRACT

Wire Arc Additive Manufacturing (WAAM) offers significant potential for enhancing steel component production. This review addresses critical challenges associated with WAAM, including defect formation, process optimization, and property enhancement. The review categorizes defects, such as porosity, cracks, and lack of fusion, and correlating them with process parameters including wire feed rate and travel speed, to identify key factors influencing component quality. The existing literature reveal that porosity can reduce tensile strength by 15–20 % and fatigue life by up to 50 %, while cracks can lead to a strength reduction of up to 30 %. Strategies for mitigating these defects, including process optimization, post-processing techniques, and emerging technologies, are discussed. Specifically, strategies to control heat input, reduce residual stresses, and refine microstructure have been shown to significantly improve build quality, mechanical properties, and overall performance of WAAM-produced steel component. This review provides valuable insights for industry practitioners for overcoming existing challenges and advancing the application of WAAM in steel production.

1. Introduction

Additive manufacturing (AM), a revolutionary fabrication process, has emerged as a powerful tool for creating complex components layer-by-layer without the constraints of traditional subtractive methods [1–4]. This technology offers unprecedented design freedom, enabling the production of intricate geometries and customized parts that were previously unattainable [5,6]. AM's potential for rapid prototyping, repair, and tool manufacturing has garnered significant attention in various industries [7,8].

The steel industry has embraced AM as a means to enhance product development, reduce material waste, and improve component performance. Mild steel, in particular, has proven to be a suitable feedstock for AM processes due to its availability, cost-effectiveness, and well-

established material properties. By leveraging AM techniques, the steel industry can unlock new opportunities for creating high-value components with tailored properties and complex geometries.

Steel, a ubiquitous ferrous alloy, is renowned for its exceptional tensile strength, ductility, and cost-effectiveness, making it an indispensable material in engineering applications [9]. Mild steel, a variant with a low carbon content, offers particular advantages due to its malleability and the potential for precise microstructure control through deposition parameters and alloying adjustments [10]. This versatility has led to its extensive use across sectors such as construction, maritime, oil and gas, wind energy, and automotive [11–14].

AM technology incorporates components like feedstock, motion systems, and heat sources to cater to diverse applications [15]. The heat source in AM can be an arc [16,17], electron beam [18,19], or laser

Abbreviations: AM, additive manufacturing; BJ, binder jetting; BOM, beads overlapping model; BTF, buy-to-fly ratio; CAD, computer aided design; CMT, cold metal transfer; CMT-PADV, cold metal transfer with monitored short-circuiting; CRM, critical raw material; DED, directed energy deposition; FE, finite element; GMAW, gas metal arc welding; GPR, Gaussian process regression; GTAW, gas tungsten arc welding; HAZ, heat-affected zone; HHHT, high heat input–high interlayer temperature; HI, heat input; LHHT, low heat input–low interlayer temperature; MAM, metal additive manufacturing; MBO, multiple-bead oscillation; PAW, plasma arc welding; PBF, powder bed fusion; PBT, powder-bed technologies; RSM, response surface methodology; SBHH, single-bead high-heat; SBLH, single-bead low-heat; SEM, scanning electron microscopy; SL, sheet lamination; SLSP, single-layer single-pass; SW, surface waviness; TOM, tangent overlapping model; TS, travel speed; UTS, ultimate tensile strength; WAAM, wire arc additive manufacturing; WFS, wire feed speed; XRD, X-ray diffraction.

* Corresponding author.

E-mail address: mohamed_hashem@eng.kfs.edu.eg (M. Dekis).

<https://doi.org/10.1016/j.rineng.2025.104657>

Received 30 May 2024; Received in revised form 27 October 2024; Accepted 16 March 2025

Available online 17 March 2025

2590-1230/© 2025 Published by Elsevier B.V. This is an open access article under the CC BY-NC-ND license (<http://creativecommons.org/licenses/by-nc-nd/4.0/>).

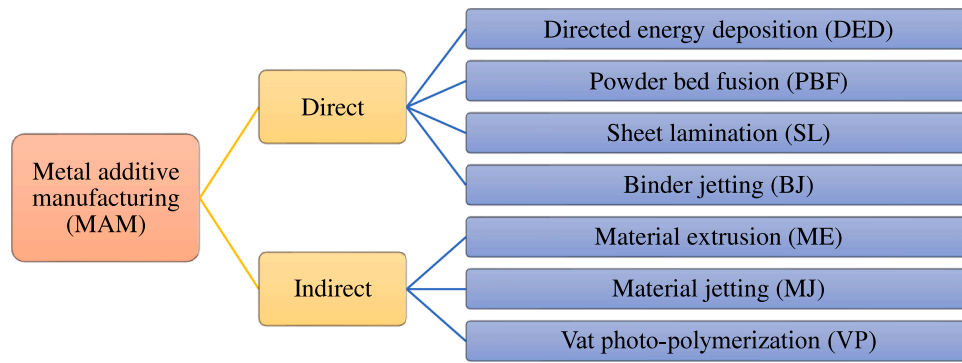


Fig 1. Classification of MAM according to EN ISO/ASTM 52921 (2015) standard [24].

beam [20–23], while feedstock materials include powder, wire, or sheet metals [24].

Metal additive manufacturing (MAM) can be categorized as direct MAM and indirect MAM as presented in Fig. 1 based on EN ISO/ASTM 52921 (2015) standard [24]. Indirect MAM involves applications like material extrusion, material jetting, and vat photo-polymerization, which are used to create tools or master patterns for conventional manufacturing techniques [25]. On the other hand, direct MAM techniques such as directed energy deposition (DED), powder bed fusion (PBF), sheet lamination (SL), and binder jetting (BJ) directly create final metal products [26,27]. Indirect MAM is closely associated with traditional production methods for non-metallic materials [28,29].

Wire Arc Additive Manufacturing (WAAM) is a specialized form DED that utilizes an electric arc as a heat source to melt and deposit a metal wire layer-by-layer, creating three-dimensional objects [30,31]. While the underlying principle of arc welding has been employed for centuries, the integration of computer numerical control (CNC) technology in recent decades has transformed WAAM into a sophisticated additive manufacturing process [32].

A WAAM system typically consists of a controlled motion system, a power supply for the electric arc, and a wire feed mechanism. The process begins with a digital design, which is then converted into a series of cross-sectional slices. Each layer is sequentially deposited by melting the wire with the electric arc and guiding the molten material onto the substrate [33,34]. This additive approach enables the creation of complex geometries with intricate details that would be challenging or impossible to produce using traditional manufacturing methods [15, 35].

WAAM has emerged as a compelling choice for the production of steel components due to its ability to achieve a balance between high deposition rates, material versatility, and geometric complexity. Compared to other AM techniques, WAAM often offers lower capital investment and operational costs, making it an attractive option for various industries [36,37].

WAAM allows for a 75 % decrease in critical raw material (CRM) consumption, as well as a 40 % to 60 % reduction in production times as compared to machining, according to the component size and geometry [15,38]. Another benefit of WAAM over other metal additive techniques, including powder-based techniques, is its cheap capital and raw material costs [39]. When compared to other AM technology such as powder-bed technologies (PBT), the WAAM process is thought to be much more appealing and economical. This is demonstrated by the energy consumption, which is 90 % less than PBT. Further, the cost of manufacturing, which comprises raw materials cost. Besides, the size of components, which are not just restricted to celled printing [40,41]. In the WAAM process, the raw material is deposited at a deposit rate of approximately 9.6 kg/hr., which is much more than 0.6 kg/hr. reached through conventional PBT methods. Almost any substance that is available as welding wire, such as steel, aluminum, titanium, and alloys based on nickel, may be used in WAAM [42–46].

Table 1
Recently published review articles.

Ref. no.	Specific Material	Building Technique	Defects	Quality improving	Microstructure and mechanical properties
[52]	Magnesium	✓	✓	×	✓
[53]	Various	✓	✓	✓	×
[54]	Various	✓	×	×	×
[55]	Steel, Ni based alloy, aluminum, titanium, and high entropy alloys.	✓	×	×	✓
[56]	Steel	×	×	×	✓
[57]	Stainless steels	✓	✓	×	✓
[58]	Magnesium alloys	✓	✓	×	✓
[59]	Various	✓	✓	✓	×
[43]	Various	✓	✓	✓	×
[60]	Nickel aluminum bronze (NAB)	✓	×	×	✓
[61]	Magnesium alloys	✓	×	×	✓
[62]	Various	✓	✓	✓	×
[63]	Various	✓	×	×	✓
[64]	Aluminum	✓	✓	✓	×
[65]	18 % nickel Maraging steels	✓	×	✓	✓
Current Work	Steel	✓	✓	✓	✓

WAAM offers the flexibility to fabricate steel alloy parts of various sizes, depending on the welding equipment [47]. Key parameters such as electric current, wire feed speed (WFS), and travel speed (TS) can be precisely controlled in WAAM [48,49], exerting a significant influence on the microstructure and mechanical properties of the manufactured steel products [50,51]. Additionally, the proper selection of the building technique and effective elimination of existing defects are crucial for achieving high-quality components.

This review aims to comprehensively explore the current state-of-the-art in Wire Arc Additive Manufacturing (WAAM) for steel alloys. By analyzing the existing literature, this review seeks to identify and assess the primary challenges hindering the widespread adoption of WAAM in the steel industry. Furthermore, it explores recent advancements and emerging techniques developed to address these obstacles. Through a systematic investigation of defect types, root causes, and mitigation strategies, this review provides valuable insights into enhancing the quality, efficiency, and overall performance of WAAM-

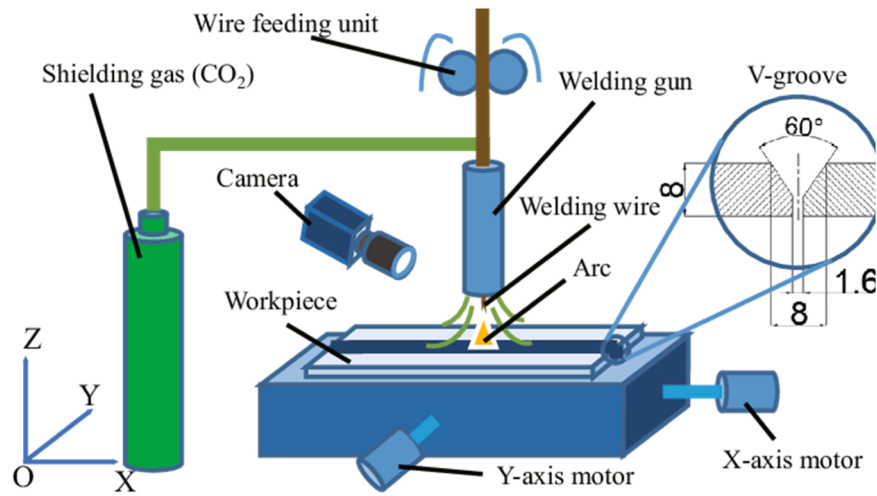


Fig. 2. Schematic diagram of the GMAW process [75].

produced steel components (see Table 1).

2. WAAM techniques of steel alloys

WAAM encompasses several techniques for fabricating steel alloys, including gas metal arc welding (GMAW), gas tungsten arc welding (GTAW), and plasma arc welding (PAW) [66,67]. These techniques offer the ability to create large, complex, and high-quality steel components for various industrial applications. Researchers and manufacturers continue to explore and improve these techniques to improve the performance and efficiency of steel WAAM. The selection of the appropriate WAAM process involves considering factors such as welding technique, process variables, shield gas, wire, and motion [68–71].

The materials employed in WAAM of steel are critical determinants of the final product's properties. Primarily, steel alloys serve as the base material, providing the structural foundation for the component. The filler wire, typically composed of a similar or compatible steel alloy, is melted and deposited layer-by-layer to form the desired geometry. Shielding gases, such as argon or carbon dioxide, are essential to protect the molten metal from atmospheric contamination, ensuring weld quality. The selection of these materials is influenced by factors including desired mechanical properties, corrosion resistance, cost, and process compatibility. For instance, low-carbon steel wires are commonly used for general construction applications, while stainless steel wires might be preferred for components requiring corrosion resistance [72].

2.1. WAAM techniques utilizing GMAW

GMAW is a core process in WAAM, involving the formation of an electric arc between a consumable electrode wire and the substrate metal. Typically, the wire is held at a near-perpendicular angle (approximately 90 degrees) to the substrate for optimal metal transfer. In single-wire configurations, torch rotation is generally unnecessary, enabling unrestricted movement of the deposition head [68,73]. Fig. 2 illustrates a simplified schematic of the GMAW process, highlighting the key components and their interactions [74].

GMAW encompasses various metal transfer modes, each with distinct characteristics. Globular transfer is characterized by large, spherical droplets that detach from the wire end and transfer to the weld pool. Short-circuiting transfer involves frequent short circuits between the wire and the workpiece, resulting in small metal droplets. Spray transfer produces a fine spray of molten metal droplets, suitable for high-deposition rates. Pulsed spray transfer combines elements of short-circuiting and spray transfer, offering control over droplet size and

deposition rate. CMT stands for an advanced method of metal transfer that enhances the GMAW process over short-circuit conditions. It relies on controlled dip transfer, wherein the wire electrode changes continuously at high frequency after each short circuit event. This controlled motion allows the previously deposited metal droplet to cool before the next one is added. CMT's advantages include rapid deposition rates and low heat input (HI), making it highly suitable for various AM applications, particularly for steel components [76–78].

2.2. WAAM techniques utilizing GTAW

To generate the weld deposit in GTAW, a non-consumable tungsten electrode serves as the heat source, while a separate wire is supplied for the material deposition. The orientation of the wire feed during the deposition process significantly influences material transfer and the quality of the deposition. A mathematical model has been developed to optimize the location and direction of the wire feed, aiming to achieve optimal deposition accuracy [79].

The gap between the shielding nozzle and the substrate varies based on the arc length. To promote effective oxidation-reduction, a gas nozzle can be utilized to facilitate the development of laminar flow in the shielding gas [80–82]. This laminar flow plays a crucial role in ensuring proper shielding during the welding process, contributing to improved deposition quality and reduced oxidation.

2.3. WAAM techniques utilizing PAW

The PAW within the realm of WAAM represents a notable advancement in the field of additive manufacturing. PAW, characterized by its concentrated energy and high welding speeds, offers a host of benefits that can be harnessed to elevate the capabilities of WAAM processes. The precision and localized energy delivery intrinsic to PAW make it particularly well-suited for fabricating intricate and intricate structures, thereby expanding the design possibilities for complex components. The controlled and concentrated HI of PAW ensures efficient material fusion, leading to enhanced layer bonding and improved overall part integrity. By utilizing PAW, the WAAM process gains the advantage of reduced heat-affected zones and minimized thermal distortion, resulting in components with improved dimensional accuracy and reduced residual stresses [59]. This adaptability extends across diverse material types and thicknesses, further bolstering the versatility of PAW for WAAM applications. As additive manufacturing continues its trajectory toward industrial integration, the incorporation of PAW technology holds immense potential for elevating the precision, quality, and efficiency of additive manufacturing processes.

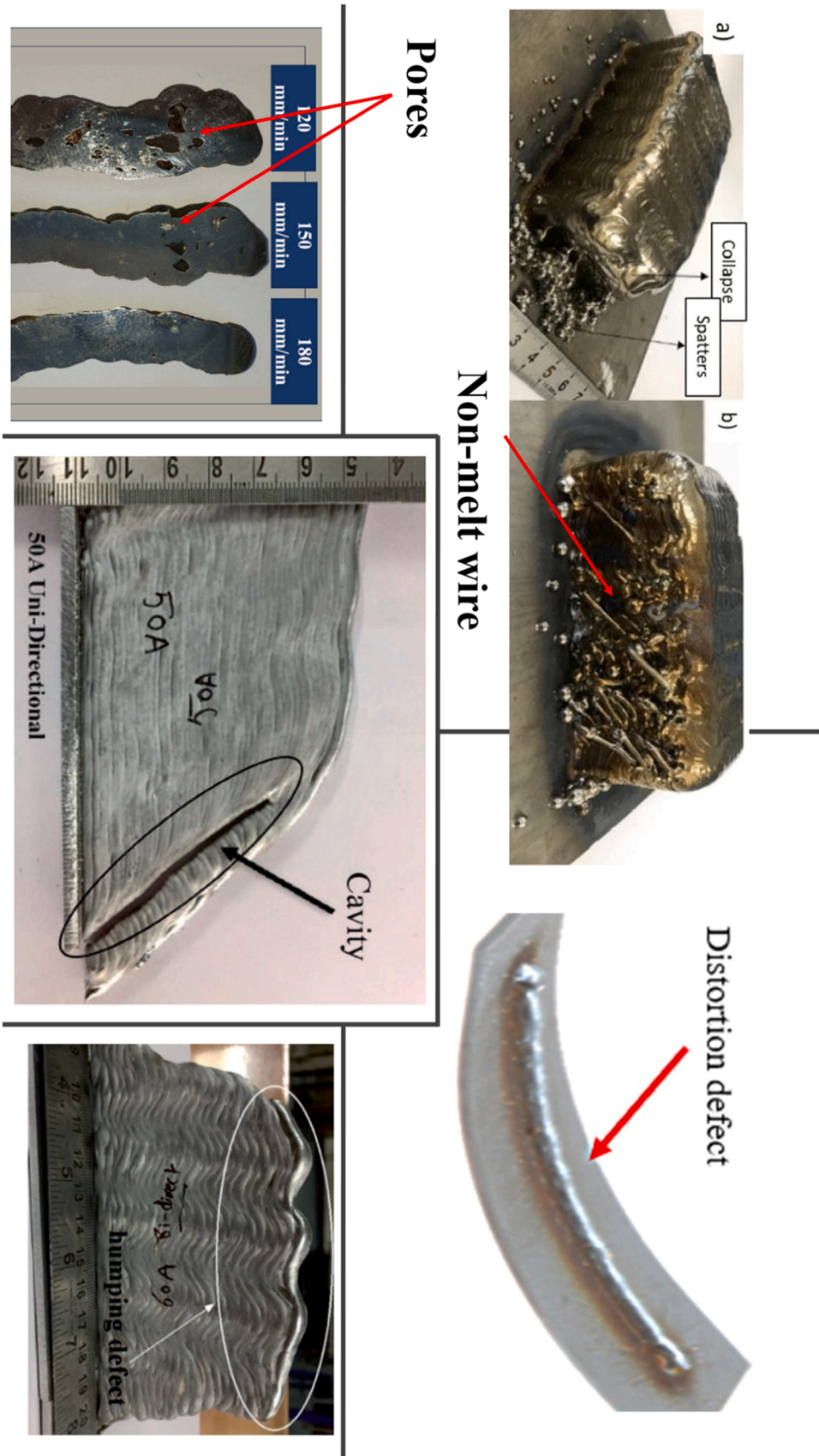


Fig. 3. Common defect types encountered in WAAM [1,93–95].

3. Challenges in wire arc additive manufacturing of steel

3.1. Material challenges

Material challenges pose significant hurdles in the successful implementation of WAAM for steel components. The inherent variability in material properties, such as chemical composition and microstructure, can lead to inconsistencies in the additive manufacturing process. Precise control over these properties is essential to achieve desired mechanical characteristics. Moreover, selecting suitable alloys and ensuring their compatibility with the WAAM process is crucial. Issues related to alloying elements, solidification behavior, and thermal stresses can impact the final product's quality. Metallurgical challenges, including porosity, microstructural defects, and residual stresses, often arise due to the rapid solidification rates and thermal gradients inherent in WAAM. Addressing these material-related challenges is imperative for advancing the technology and producing reliable steel components [83].

3.2. Process challenges

Process-related challenges significantly impact the efficiency and quality of WAAM for steel components. Precise control of deposition parameters, such as WFS, TS, and arc current, is crucial for achieving desired material properties and geometric accuracy. Maintaining consistent and stable process conditions is often challenging due to variations in material feedstock, equipment performance, and environmental factors. Surface quality and roughness are critical considerations for functional and aesthetic requirements. Achieving smooth and defect-free surfaces can be demanding, especially for complex geometries. Additionally, improving build rate and productivity while maintaining acceptable quality is a persistent challenge in WAAM. Optimizing process parameters and equipment configurations is essential for enhancing the overall efficiency of the additive manufacturing process [84].

3.3. Design and simulation challenges in WAAM of steel

Design and simulation play pivotal roles in the successful implementation of WAAM for steel components. Optimizing component designs for additive manufacturing requires a departure from traditional subtractive design principles. Considerations such as build orientation, support structures, and part consolidation are crucial for maximizing part quality and minimizing costs. Accurate simulation of the WAAM process is essential for predicting thermal behavior, residual stresses, and microstructure formation. Developing reliable predictive models is challenging due to the complex interplay of process parameters, material properties, and geometric factors. Bridging the gap between design, simulation, and actual production is key to unlocking the full potential of WAAM for steel components [85,86].

3.4. Defects associated with WAAM of steel

In numerous cases, the mechanical properties of steel parts produced through WAAM are comparable to those manufactured using conventional methods [87]. WAAM is a non-equilibrium processing technique characterized by rapid cooling rates and significant thermal gradients. However, the high heat involved in WAAM can lead to complex phase transformations, non-uniform residual stresses or distortions, porosity, cracking, and subsequent degradation in corrosion resistance, mechanical behavior, and impact resistance [5,44,88–90].

These defects can arise from various sources, including improper programming approaches, unstable weld pool dynamics due to inadequate parameter settings, thermal deformation resulting from heat accumulation, environmental influences, and other mechanical faults [91]. To illustrate these defects, Fig. 3 depicts common defect types encountered in WAAM, such as porosity, lack of fusion, distortion, and

Table 2
Common defects of steel components manufactured by WAAM.

Authors & Ref.	Material	Characterization techniques	Process	Defect					Impacts	
				Surface finish	Substrate adherence	Oxidation	Delamination	Cracking		Porosity
Yang, He et al.[96]	H08Mn2Si steel	Using double electrode gas metal arc welding	DE-GMAW	Waviness	Good	Nope	Nope	Nope	low	<ul style="list-style-type: none"> As the bypass current increased, the width of the deposited part decreased, while the height increased proportionally at the same deposition rate. The utilization coefficient of materials saw a notable increase of approximately 13 % when DE-GMAW was employed for depositing thin-wall components within a specific range of bypass current. Higher currents, above 200 A, lead to instability and pool overflow, potentially causing part collapse. Optimal appearance is achieved at 100–180 A, with reduced HI.
Xiong, Zhang et al.[97]	Copper-coated steel	Investigating how the arc current, deposition velocity, and heat input impact the overall appearance of deposited parts	GMAW	GMAW	Good	Light	Nope	Nope	Nope	<ul style="list-style-type: none"> Manufacturing a mild steel-silicon bronze bimetal part through GMAW with a single-pass multi-layer model is feasible. Tensile strength reaches 305 MPa, and fracture occurs near the center of the bronze side, indicating a strong connection. No welding defects were found near the interface between the two metals Hardness near the interface matched bulk material. The bond strength between the two metals is comparable to the tensile strength of individual weld metals, suitable for mechanical applications.
Liu, Zhuang et al.[98]	Steel-bronze bimetal	Using bimetallic materials	GMAW	Smooth	Good	Nope	Nope	Nope	Nope	
Abe and Sasahara [99].	Intermetallic Fe/Al	Dissimilar metal deposition	GTAW	Medium-poor	Medium	Serious	Nope	Yes	High	

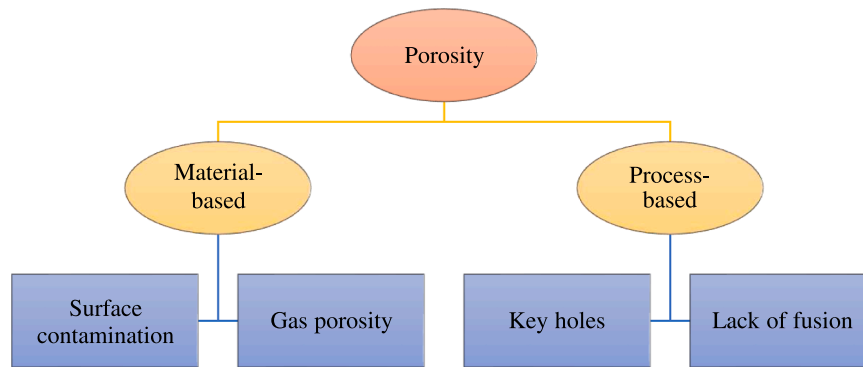


Fig. 4. Classification of porosity.

cracks. These defects, as outlined in Table 2, can significantly impact the material properties and component performance [38,92].

The selection and control of process parameters are critical in mitigating defect formation during WAAM. WFS, a pivotal parameter, influences HI and material deposition. Excessive WFS can lead to increased HI, resulting in larger melt pools, higher porosity, and potential hot cracking. Conversely, low feed rates may cause insufficient HI, leading to lack of fusion and cold laps. TS also significantly impacts defect formation. High TS can result in shallow penetration, lack of fusion, and increased porosity, while low speeds may cause excessive HI and increased porosity. Arc current and voltage directly influence HI and melt pool size. Excessive values can lead to increased porosity and reduced mechanical properties, while insufficient values can result in poor bead formation and lack of fusion. Gas flow rate is essential for shielding the weld pool. Excessive flow rates can cause rapid cooling and increased thermal stresses, while insufficient flow rates can lead to oxidation and porosity. Other parameters such as torch angle and powder injection also play roles in defect formation. By carefully optimizing these parameters, it is possible to minimize defect occurrence and enhance the overall quality of WAAM components.

3.5. Residual stress and distortion

Residual stress and distortion are inherent challenges in the WAAM process, similar to other additive manufacturing and thermomechanical processes [100]. Residual stress refers to stresses that persist in a material even after external forces have been removed, which is responsible for the distortion and damage of components [101]. The layer-by-layer nature of WAAM results in a complex thermal cycle with melting, remelting, and reheating of the material. The non-equilibrium conditions, characterized by rapid cooling rates and thermal gradients, lead to the presence of residual stresses [102–104]. These residual stresses can lead to part deformation, layer delamination, reduced geometric tolerance, and compromised mechanical properties, including fracture resistance and fatigue performance [89,105–108]. Managing residual stresses is crucial for ensuring the quality and performance of WAAM components [109].

The residual stresses can be assessed using destructive and non-destructive techniques. Destructive methods, such as ring-core drilling, serial sectioning, and hole drilling, rely on mechanical stress relaxation. Non-destructive approaches involve measuring lattice spacing using diffraction methods, as well as using the speed of sound and Barkhausen noise techniques [106,110–112].

3.6. Porosity

Porosity refers to the presence of gas trapped in the components leading to the formation of pores. It is considered another crucial aspect in WAAM to ensure optimal component quality. The porosity negatively affects the mechanical characteristics of fabricated components,

including fatigue resistance, anisotropy, oxidation, and corrosion resistance [113,114]. The types and shapes of pores in components can significantly affect their characteristics. Clusters or irregularly shaped pores are considered more detrimental to mechanical properties compared to spherical pores, especially when they are oriented perpendicular to the loading direction. These types of pores can lead to reduced strength and structural integrity of the components, highlighting the importance of minimizing their presence during the WAAM process [115–118].

The porosity in WAAM can be categorized into two main types: material-based porosity and process-based porosity, as shown in Fig. 4. Material-based porosity is related to the feedstock, which includes the wire and substrate. Surface contaminants like oils, dust, grafting, hydrocarbon mixtures, and moisture present in the feedstock can be challenging to be eliminated. During the process, the molten pool can quickly absorb these contaminants, leading to the formation of porosity during solidification [119–121].

Process-based porosity, on the other hand, can result from poor path design or an unstable deposition procedure. One significant cause of process-based porosity is the formation of keyholes, which occurs due to the high energy density during deposition, leading to gas trapping and localized vaporization. Keyholes are relatively large pores, either horizontally circular and elongated in the building direction or with a broader top than the bottom [122–124]. Lack of fusion is another form of process-based porosity that arises from inadequate energy input or insufficient melt pool penetration into the substrate.

Measurement of porosity/density in wire arc additively manufactured components can be achieved using various methods, including gas psychrometry, hard X-rays at synchrotron facilities, X-ray micro-computed tomography (μ -CT), image analysis of metallographic cross-sections, ultrasonic pulse-echo velocity measurements, and the Archimedes technique. These techniques provide valuable insights into the porosity and density distribution within the components, aiding in the assessment of their quality and performance [122,125,126].

To minimize porosity in produced parts through WAAM, innovative techniques like pulsed GMAW or Cold Metal Transfer with monitored short-circuiting (CMT-PADV) can be employed. Ensuring the use of high-quality shielding gas, gas-tight seals, short pipe lengths, and non-organic pipework during fabrication is crucial. Additionally, using high-quality feedstock, modifying the profile of the deposited bead, implementing post-processing heat treatment, and maintaining rigorous temperature control and monitoring during metal deposition are recommended steps, all of which come after cleaning the wire and substrate. By adopting these measures, the porosity formed in fabricated components can be significantly reduced, leading to improved component quality and performance [106,127].

Numerous studies [128–133] have explored porosity in WAAM, using simulations, microstructural analysis, and non-destructive testing to understand and mitigate it. By linking process parameters, material properties, and porosity levels, these studies established guidelines for

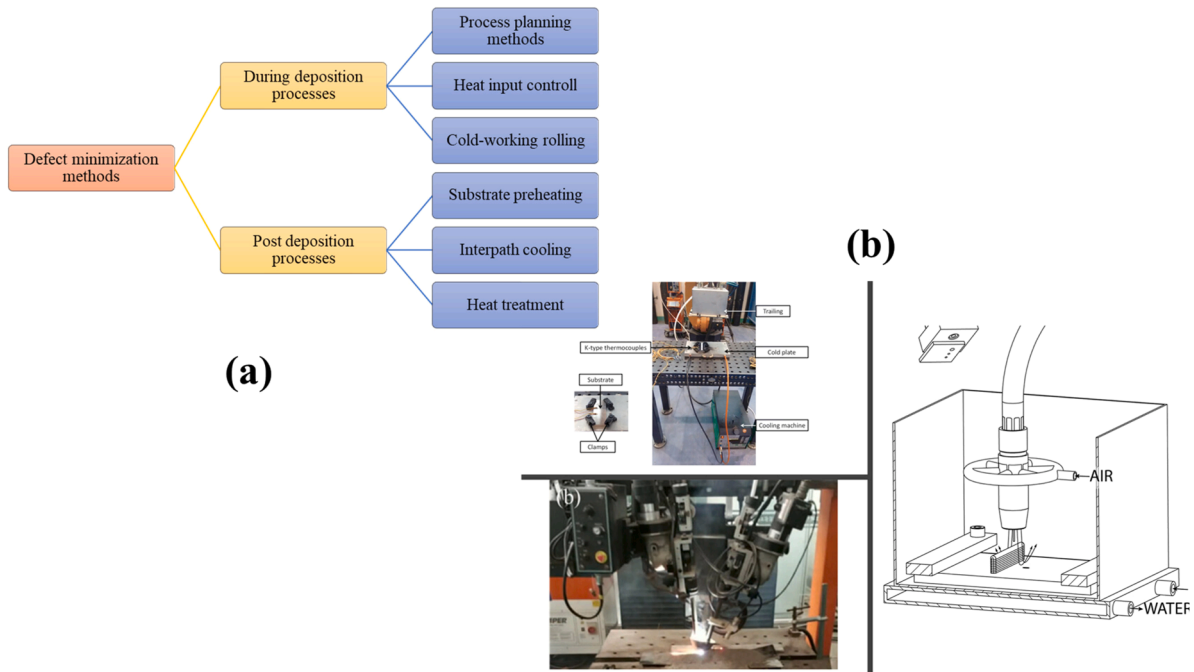


Fig. 5. (a) Some of employed methods for defects minimization and (b) examples of defects minimization methods [146,147].

minimizing porosity. Such as adding additives like SiC powder [128], using convolutional neural network algorithm for the purpose of analyzing volumetric images [130], and oscillating the arc [131].

Porosity remains a critical challenge in WAAM, significantly impacting component performance. Originating from gas entrapment, shrinkage, or lack of fusion during the solidification process, porosity can lead to a reduction in tensile strength by an average of 15–20 % [134], fatigue life by up to 50 % [135], and ductility by 10–15 % [134]. Studies have shown that porosity levels exceeding 2 % can lead to catastrophic failure.

3.7. Cracking and delamination

Cracking and delamination are two distinct defects that can occur during the WAAM process. Cracking during solidification at grain boundaries refers to the creation of shrinkage during the solidification stage of weld metal [136–138]. On the other hand, delamination occurs when the initially deposited layers separate from the baseplate between two subsequent layers. Both of these defects can compromise the structural integrity and mechanical properties of the fabricated components, highlighting the importance of effective strategies to prevent or mitigate their occurrence.

Several factors contribute to the occurrence of cracking and delamination. Variations in dissolution or precipitate production, as well as grain boundary morphology, can lead to grain boundary cracks. Solidification cracks, on the other hand, are caused by obstructions in grain flow during solidification or high stresses in the molten pool, which are influenced by the material's solidification characteristics [139,140]. Cracking may result from factors such as excessive energy supplied to the material, the nature of solidification, significant solidification shrinkage, rapid heating below the liquidus temperature, melting of certain grain-boundary precipitates, and a wide gap between the solidus and liquidus temperatures of certain alloys [89,139,141,142]. Delamination occurs when the material between layers is insufficiently melted and cannot be rectified even with post-processing treatment [143]. Understanding and addressing these factors are essential to mitigate cracking and delamination issues during the WAAM process.

To identify cracking and delamination, both destructive and non-destructive testing methods are used. Destructive tests involve cross-

sections of the metal, and cracks are examined using scanning electron microscopy (SEM). Non-destructive testing methods include magnetic particles, radiography, μ -CT, and ultrasonic testing.

Preventing the formation of cracking and delamination is essential to minimize their negative effects. Steps to prevent these defects include ensuring compatibility in printing multiples, optimizing scan strategy and component orientation during construction, reducing aspect ratios and wall thicknesses, optimizing cooling times, and preheating the substrates and the chamber [49]. These measures can help reduce the occurrence of cracking and delamination and improve the overall quality of WAAM-produced components. By implementing these preventive measures, the reliability and performance of the fabricated parts can be enhanced, making them suitable for various industrial applications.

Cracks, a critical defect in WAAM, significantly impact component performance. Originating from excessive thermal stresses, material defects, or hydrogen embrittlement, cracks can reduce strength by up to 30 % and drastically affect fatigue life [144]. Their presence acts as stress concentrators, accelerating crack propagation and leading to premature failure. A crack density exceeding 1 crack per mm^2 is often considered critical, as it renders a component unusable [145]. To mitigate crack formation, precise control over process parameters, optimization of HI, and careful material selection are essential. Post-processing techniques like stress relief and heat treatment can also contribute to crack prevention.

3.8. Methods of minimizing defects associated with WAAM of steel

The selection of the production method is pivotal in achieving the desired properties of the fabricated component. While WAAM has emerged as a promising technique for producing various metallic components, especially steel, it is still susceptible to defects that require further investigation. To address the defects outlined in the previous section, a combination of in-process and post-process strategies can be implemented. Fig. 5. illustrates a comprehensive overview of these methods.

For instance, process parameters such as WFS, TS, and arc current can be optimized to control HI and melt pool dynamics, thereby reducing porosity and lack of fusion. Post-process treatments like heat



Fig. 6. Various forming appearances with different combinations of process parameters (a) an incomplete fusion of weld toe, (b) excellent appearance (c) overflowing, and (d) hump and scallop [97].

treatment and stress relief can mitigate residual stresses and improve mechanical properties. By employing a multi-faceted approach, the occurrence of defects can be significantly reduced, leading to enhanced component quality and reliability.

3.9. Defects minimization methods during the deposition process

In this section, we delve into various methods employed to address defects in the deposition of steel components using the WAAM process. These methods encompass process planning techniques, HI control, and cold-working rolling. Process planning involves accurate slicing approaches and mathematical models to optimize process factors and predict layer thickness and yield strength. HI control ensures proper energy supply to the material, while cold-working rolling reduces residual stresses and improves mechanical properties. These techniques play a crucial role in enhancing the quality and performance of WAAM-produced steel components.

3.9.1. Process planning methods

Process planning in WAAM involves a sequence of strategic decisions with considerable impact on quality, efficiency, and success. Precise planning and optimization enhance part quality, reduce defects, and optimize the potential of this advanced manufacturing technique.

In WAAM of steel components, the initial step includes creation of 3D Computer Aided Design (CAD) model using software such as Unigraphics and SolidWorks or scanning existing models with 3D scanners [148]. These models are converted into machine code through solid, surface, and mesh technologies. Accurate slicing techniques play a pivotal role in managing deposition impacts and defects reduction. Advanced algorithms are vital for achieving high-quality WAAM. Uni-directional slicing divides CAD models into uniform thickness layers, influencing part dimensions and computation time [14,149,150]. Alternatively, multi-directional slicing segments models into 2.5D layers with constant or variable thickness [151].

Critical to WAAM process planning is selecting the optimal build direction. This parameter impacts thermal history, residual stresses, and mechanical properties of final parts. Optimization of build orientation mitigates distortion, enhances material properties, and attains desired performance attributes [152–154].

Process planners determine optimal layer thickness and deposition strategy for each build layer [76,155]. Thicker layers speed up the process but may raise defect and residual stress risks. On the other hand, thinner layers offer finer resolution but extend build times. Layer thickness's impact on quality and properties has been studied [156]. Prudent layer thickness and deposition pattern selection strikes a balance between speed and quality.

Mathematical models predicting layer thickness and yield strength were used to optimize WAAM, factoring droplet transfer mode, electric arcing mode, WFS, current intensity, and material deposition rate [101, 157,158]. Models link single and multi-bead geometries to process parameters. For instance, Suryakumar et al. developed a multi-bead deposition model considering material overflow between paths, predicting layer thickness and yield strength, and optimizing parameters for higher yield strength and lower HI [159].

Additionally, Xiong et al. compared various profile models for weld beads under different welding conditions, with the arc model showing greater accuracy for certain ratios of WFS to TS, and the parabola model being more suitable for other ratios [160]. Ding et al. introduced the "tangent overlapping model" (TOM), using parabola, cosine, and arc functions, which demonstrated higher efficiency compared to conventional flat-top overlapping models [151]. Li et al. developed the Beads Overlapping Model (BOM) and its enhanced version (E.BOM) to reduce surface roughness and prevent internal defects in WAAM-produced components caused by the spread of melted weld beads due to surface tension in the weld pool [161]. To enhance production and building quality in the multi-variable WAAM process, Gaussian Process Regression (GPR) has been employed as a reliable method for optimization. This approach has led to an improved buy-to-fly ratio (BTF), contributing to more efficient and higher-quality production of WAAM components [162,163].

Managing cooling strategies is vital to control thermal gradients, residual stresses, and distortion [164,165]. Techniques like inter-layer or inter-pass cooling regulate temperature and solidification. Cooling's impact on stress and distortion reduction has been studied. Skillful cooling optimization prevents defects and maintains material uniformity [166]. Incorporating advanced simulation and optimization tools into planning enhances effectiveness. Models predict thermal behavior, residual stresses, and distortion. Simulation tools optimize parameters iteratively, reducing trial and error [162,167,168].

Selecting base materials [169], filler wires [170], and shielding gases [171,172] is essential. Compatibility, melting points, and mechanical properties are key considerations. Material selection impacts microstructure and mechanical properties. Effective support structures prevent distortion and enhance stability. Strategic support design improves accuracy and reduces post-processing [173–175].

WAAM's success hinges on process planning. Optimizing build direction, layer thickness, scan paths, cooling, and materials improves quality, reduces defects, and enhances efficiency. Simulation and research findings enhance planning, ensuring WAAM fully delivers rapid manufacturing's benefits.

3.9.2. Heat input control

The HI is a crucial factor in the design of welding techniques [176]. It is defined as the measurement of the total delivered energy per unit length of the weld [177]. HI plays a significant role in determining the grain size in the heat-affected zone (HAZ). In general, low HI is preferred in welding as it provides finer microstructure, reduces stress, and minimizes distortion, which is commonly used for industrial applications. However, WAAM's main advantage lies in its high deposition rate and efficiency, which requires a higher HI rate, impacting the printing quality [47,178].

To ascertain an appropriate HI that fulfills WAAM criteria without inducing excessive heating that may negatively affect component properties, the following equation is utilized, denoted as HI (J/mm):

$$HI = \frac{V \times I}{TS} \times \eta \times 0.06 \quad (1)$$

Where V, I, and TS represent voltage in volts, current in amperes, and travel speed of the welding torch in meters per minute, respectively. η denotes the efficiency of the welding process, and HI is directly influenced by these process parameters. Each arc welding method has different efficiency ratings, and to facilitate comparison, all efficiency variables are related to the efficiency of submerged arc welding, with a unit conversion factor of 0.06 [179].

The examination of sample properties and their alterations under various HIs revealed significant insights [97]. Exploratory trials were conducted to establish connections between process parameters and single-layer single-pass (SLSP) outcomes. This investigation classified forming quality into four distinct types, area A: Low current, high deposit velocity - unstable arc, incomplete melting, poor surface quality as depicted in Fig. 6-a, where area C: Low deposit velocity, high current - excessive HI, pool overflow, bead wrinkles Fig. 6-c, area D: High deposit velocity, high current - irregular SLSP width and height changes, humps, and scallops due to strong arc force and droplet impact Fig. 6-d whereas area B represents the best building quality at optimum parameters. The relationship between HI in WAAM and the WFS in relation to deposited velocity on the substrate plate determines the wire feed to deposited velocity ratio, which escalates with higher HI.

In a multi-objective optimization approach, researchers focused on Bainite steel additive manufacturing used the Box Behnken design of response surface methodology (RSM) to establish a welding design matrix for trials [180]. Low heat input-low interlayer temperature (LHLT) and high heat input-high interlayer temperature (HHHT) scenarios were explored, showing that increased heat input and interlayer temperature didn't notably impact the number of layers but did influence overall passes and as-deposited austenite fraction [181]. Utilizing CMT-based WAAM technology, varying heat inputs through adjustments in WFS and TS led to changes in effective wall width, layer thickness, height, and width-to-height ratio [182,183]. These findings underscore the impact of bead geometry, interlayer temperature, solidification rate, WFS, TS, and HI on the macroscopic macrostructure, with reduced HI favoring precision and deposition speed, and all variables contributing to optimizing bead geometry [178].

Effective HI management is crucial in WAAM. HI significantly impacts the HAZ grain size and overall component properties. Low HI promotes fine microstructures, residual stresses reduction, and minimal distortion, which fits with industrial needs. However, WAAM's advantage lies in its rapid, efficient deposition, necessitating higher HI that can affect manufacturing quality. Achieving an appropriate balance between HI, process parameters, and desired component properties is crucial for optimizing WAAM outcomes.

Precise heat control is paramount in WAAM to achieve desired microstructures and mechanical properties. Rapid solidification rates and thermal gradients inherent in the process significantly influence phase transformations, grain growth, and residual stress formation. By manipulating HI through parameters such as WFS, TS, and arc current, it

is possible to control the cooling rate and solidification path.

A slower cooling rate, achieved by reducing TS or increasing HI, can promote the formation of coarser grains, leading to increased toughness but potentially reduced strength. Conversely, rapid cooling rates can result in finer grains, enhancing strength but potentially compromising ductility. The formation of specific phases, such as martensite or bainite, is also influenced by cooling rate.

Residual stresses, arising from thermal gradients, can significantly impact component distortion and fatigue life. By optimizing HI and cooling conditions, it is possible to minimize residual stress formation. Techniques like preheating and post-weld heat treatment can further aid in stress relief.

3.9.3. Cold work rolling

Cold work rolling serves as an effective method for relieving tension in steel components, applicable to both thin steel sheet welds and steel WAAM. Inter-pass rolling has demonstrated its ability to refine grain structure, mitigate distortion, and reduce residual stresses [83,101,184]. A technique involving layer-wise rolling of steel WAAM components has been explored, using profiled or slotted rollers to counteract defects. While both rollers diminished distortion and surface roughness, the slotted roller exhibited superior performance, resulting in decreased residual stresses and enhanced grain refinement [185]. A hybrid deposition and micro-rolling method was innovatively used to address deep penetration and temperature gradient-related issues, achieving surface flattening and uniform deformation [186]. Additionally, the impact of post-deposition side rolling on surface waviness (SW) was investigated, showing that increased rolling loads decreased SW, minimizing stress concentration and enhancing fatigue life [187].

Cold work rolling offers potential for enhancing steel WAAM components, including residual stresses reduction, distortion control, porosity minimization, microstructural enhancement, and improved geometry. However, application scope may be limited to specific designs, considering research mainly focuses on basic geometric pieces and inter-pass rolling might extend lead times and potentially impact WAAM's rapid deposition advantage [188].

The impact of cold work rolling on steel structures manufactured by WAAM is discussed by Liu et al. [189]. They underlined that cold work rolling induces plastic deformation, refining grain structures and eliminating residual stresses, enhancing mechanical properties like hardness, tensile strength, and fatigue resistance. The process fosters dislocations and sub grains within the microstructure, bolstering strength mechanisms. The findings obtained by Wang et al. [190] show that cold work rolling increases dislocation density and forms dislocation walls, triggering strain hardening and higher yield strength. Grain structure refinement increases grain boundaries, obstructing dislocation motion and enhancing strength.

Excessive cold work rolling presents challenges as intense plastic deformation, when controlled, refines grain structures and improves properties; however, excessive strain accumulation can lead to defects, heightened dislocation density, localized stress, and microstructural instabilities [191]. Despite these challenges, over-cold work rolling can also customize WAAM deposit microstructure and properties. Controlled rolling parameters, such as reduction ratio and annealing conditions, mitigate excessive deformation. Optimization of cold work rolling can achieve desired microstructural features while avoiding detrimental outcomes.

Over cold work rolling's impact on WAAM deposits is complex. Excessive plastic deformation potentially improves properties but introduces challenges like defects and instabilities. Balancing optimized properties and avoiding negatives is vital. Understanding deposited material behavior is key for successful implementation.

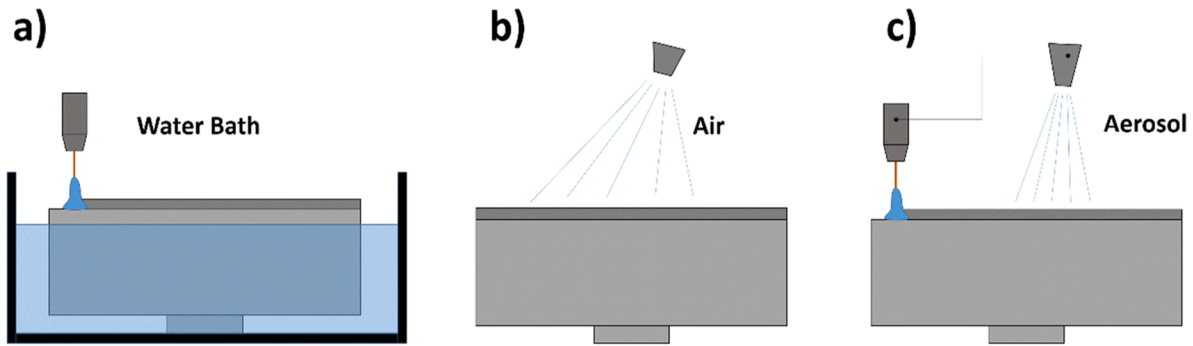


Fig. 7. (a) water path cooling, (b) pressured air cooling, and (c) aerosol cooling [164].

3.10. Defect minimization post-printing process methods

3.10.1. Substrate preheating

Substrate preheating stands as a pivotal technique in WAAM, elevating the base material temperature before additive layer deposition. This strategy exerts profound influence on microstructural evolution, thermal behavior, residual stresses, and mechanical properties of components, all while enhancing final product quality and additive manufacturing efficiency. By addressing challenges linked to heat stress and thermal gradients during additive deposition, substrate preheating mitigates uneven thermal distribution, gradients, and resultant material stresses stemming from localized heating and cooling cycles induced by welding arc HI. Elevating the base material's initial temperature through preheating effectively narrows the temperature difference between the molten weld pool and the substrate, further enhancing the overall effectiveness of the WAAM process.

Crucial to substrate preheating is the interplay between preheating temperature and solidus temperature. Optimal preheating conditions strike a delicate balance between promoting favorable microstructural changes and preventing undesired phase transformations. Leveraging advanced computational tools, such as finite element analysis and machine learning algorithms, researchers identify precise preheating parameters that maximize benefits while minimizing drawbacks. These tools provide valuable insights, offering valuable guidance to ensure optimal substrate preheating and its positive impact on the additive manufacturing process.

Substrate preheating effectively addresses heat stress and component cracking in WAAM [101,143]. Bai et al. [192] explored induction heat coils' impact on the weld pool, observing reduced residual stresses and uniform HI via simulations and experiments. In GMAW-based AM, Xiong et al. [193] used 3D finite element modeling to analyze thermal behavior, identifying optimal preheating temperatures (400–600°C) that mitigate thermal stress and cracking. Wu et al. [194] utilized machine learning to predict residual stress effects, underscoring substrate preheat temperature's significance among process parameters. Their study highlighted preheating-solidus temperature interplay in

influencing residual stresses.

Substrate preheating emerges as a vital technique in WAAM, offering enhanced component quality, curbing residual stresses, and improving mechanical properties. By strategically raising the base material's temperature, manufacturers can optimize the microstructural evolution and thermal behavior of fabricated components, ultimately enhancing their overall performance and efficiency.

3.10.2. Inter-path cooling

Inter-path cooling in WAAM involves the deliberate implementation of cooling mechanisms between adjacent deposition layers. As the weld pool solidifies from its molten to solid state, controlled cooling moderates thermal gradients, ensuring gradual cooling of the deposited material. This approach prevents abrupt thermal contraction, curbing associated residual stresses stemming from rapid cooling rates. A key advantage is its efficacy in averting excessive heat accumulation, particularly in multi-layer builds. In the absence of proper cooling measures, cumulative HI from successive paths can lead to localized overheating and heightened thermal gradients, potentially inducing distortion or defects in the final part. Techniques like directed air or water cooling keep material temperature within a desirable range, safeguarding mechanical properties and structural integrity. Cooling strategies can vary, involving adjustments to process parameters, traverse speed, or external cooling mechanisms. Selection depends on factors like deposited material, deposition rate, and part geometry. Computational simulations and modeling predict temperature distribution and optimize cooling methods for specific applications [47,195].

Extensive research has delved into understanding how inter-pass temperature impacts component attributes in the WAAM process. This variable significantly influences metallurgical properties, molten pool dimensions, structural defects, and the risk of thermal overheating in components [196]. Maintaining meticulous control over inter-pass temperatures is essential to prevent cracking and achieve the desired grain structure formation. Optimal inter-pass temperatures typically range from 50 to 120°C, contingent upon material properties and experimental setups [164,197–199].

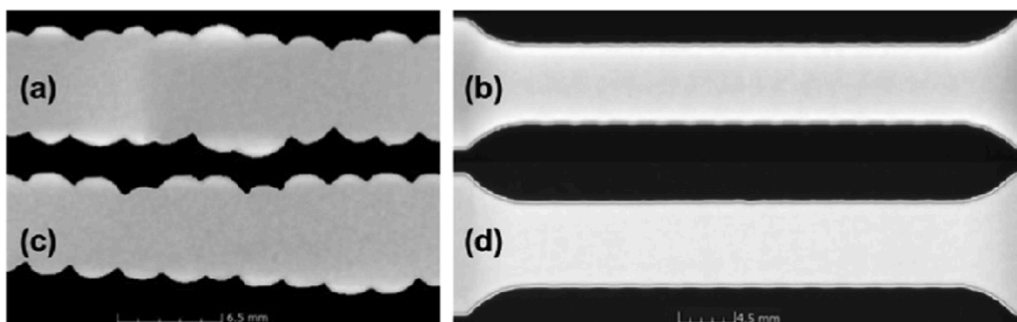


Fig. 8. X-Ray CT photographs for (a-b) 30 s dwell time wall and (c-d) 60 s dwell time wall [200].

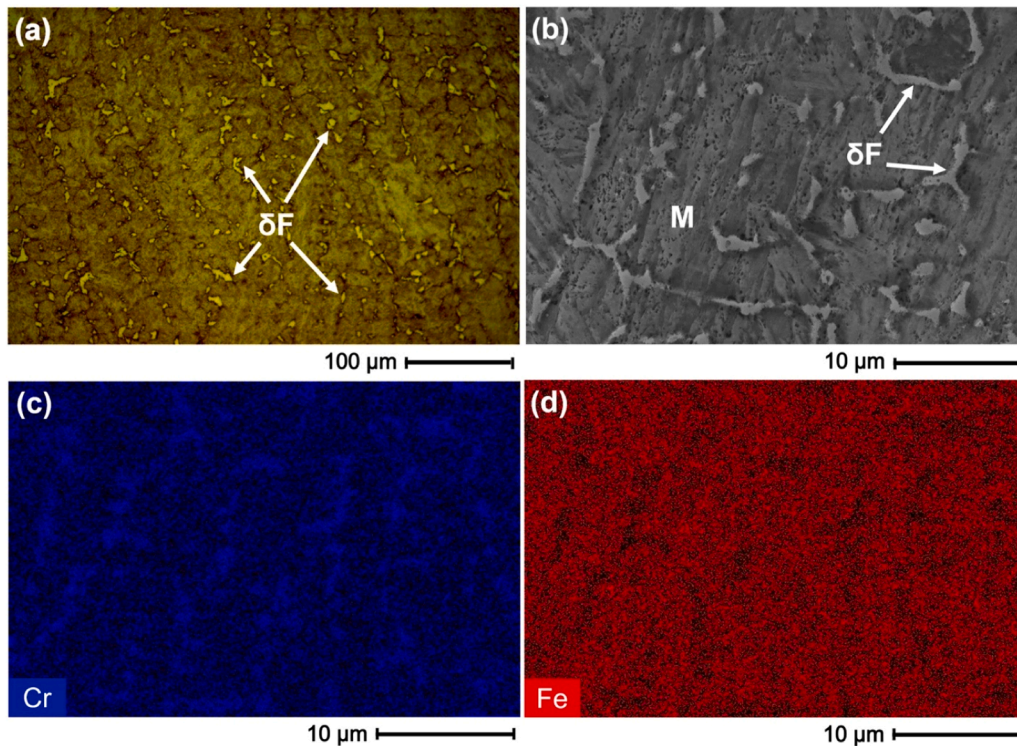


Fig. 9. (a) optical microscope (OM) image, (b) scanning electron microscope (SEM) image, (c) Cr EDS elemental maps, and (d) Fe EDS elemental maps [207].

In a comparative study [164], diverse cooling methods were investigated, including aerosol, high-pressure air, and water bath cooling (as illustrated in Fig. 7). These approaches exhibited substantial reductions in cooling rates and durations compared to the reference uncooled weld. Water bath cooling emerged as the most effective method, while high-pressure air cooling faced constraints due to disturbances in the shielding gas cloud, limiting its application until after welding layer deposition. Conversely, aerosol cooling displayed promise, causing minimal interference with the shielding gas cloud and enabling in situ application during deposition. An intriguing proposition involved combining high-pressure air cooling with aerosol cooling to minimize process idle time and influence phase change behavior.

An alternative inter-pass temperature control approach was pursued [146], involving the use of an IR pyrometer to remotely measure the final layer's temperature. By pausing deposition after each layer, inter-pass temperature was maintained below a predefined threshold, with cooling facilitated through water and high-pressure air systems. This approach achieved a consistent inter-pass temperature of 150°C during deposition, enhancing dimensional accuracy of printed items compared to other methods.

The effect of inter-pass cooling periods on the microstructure of stainless steel (SS308L) walls produced using WAAM was examined [200]. In experiments utilizing unidirectional depositing techniques, two SS308L walls were fabricated with inter-pass cooling durations of 60 and 30 seconds between successive layers. X-ray CT scans of produced samples (as shown in Fig. 8) revealed no signs of severe defects like macro porosity or cracks. Notably, different inter-layer idle periods yielded no observable discrepancies in microstructure development between the constructed walls.

To evaluate air jet impingement cooling's effectiveness during WAAM [201], a hybrid numerical-experimental approach was employed. Finite Element (FE) heat transfer analysis provided temperature distribution insights during deposition. This study demonstrated air jet impingement cooling effectively reduced substrate temperatures across studied setups, consistent with previous findings [202]. Although extending the idle period from 30 to 120 seconds during air jet

impingement testing yielded no further substrate temperature reductions, adopting a 10-second idle period revealed partial temperature decrease in the substrate. This suggests air cooling efficiency is process-dependent and influenced by jet conditions and workpiece size.

Optimal inter-pass temperature control is vital for enhancing WAAM component quality, impacting metallurgical properties and structural integrity. Maintaining suitable inter-pass temperatures, around 50 to 120°C, prevents cracking and promotes desired grain structures. Methods like water bath and aerosol cooling improve cooling rates, while remote temperature measurement and control enhance consistency. Microstructure studies and air jet cooling evaluation highlight the significance of controlled cooling in WAAM.

3.10.3. Heat treatment

In the WAAM approach, post-process heat treatments play a pivotal role in diminishing residual stress, controlling hardness, and enhancing material strength [203–205]. The choice of appropriate heat treatment procedure hinges on factors like temperature, deposited material, and the specific AM technique employed. Inadequate heat treatment may escalate the risk of cracks upon mechanical loading [205,206]. Nonetheless, suitable post-process heat treatments have exhibited substantial enhancements in mechanical strength, particularly notable in steel alloys [127]. The ensuing sections will delve into the direct influence of heat treatment on the mechanical properties of WAAM products.

Achieving near-flawless bead geometry in WAAM products mandates meticulous optimization of torch tool paths and process parameters. Tackling these optimization challenges entails considerations of factors such as HI, WFS, TS, current, and voltage's impact on material properties, alongside inter-pass temperature and path planning's effects on deposition characteristics. A comprehensive understanding of the interplay between build attributes and process parameters is essential for curbing defects, mitigating surface irregularities, and alleviating residual stresses in WAAM components.

The integration of post-process heat treatments enhances the mechanical properties of WAAM components, while the pursuit of near-flawless bead geometry demands a meticulous optimization approach

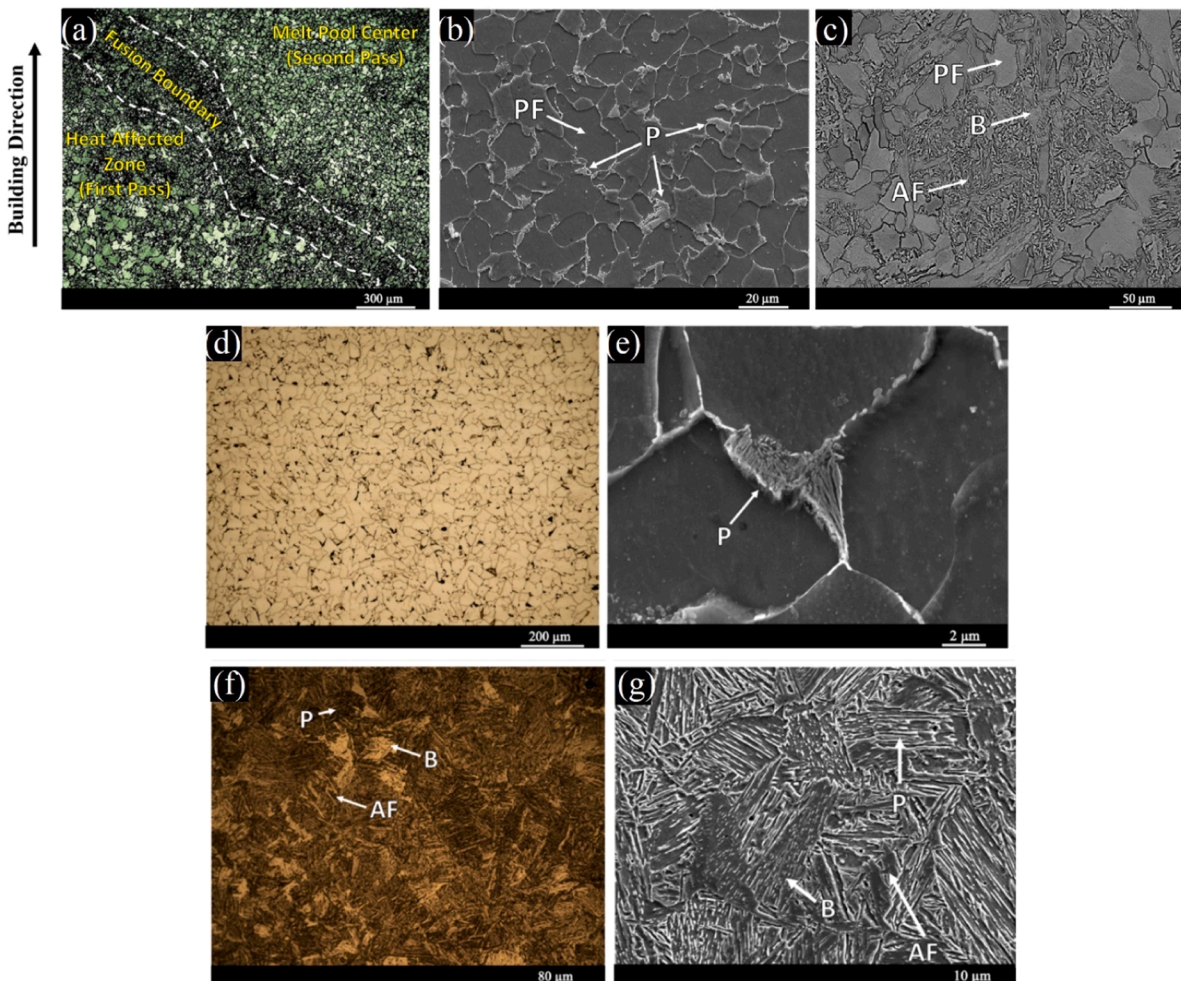


Fig. 10. (a) as- fabricated sample low magnification OM, (b) melt pool center higher magnification SEM, (c) fusion boundary higher magnification SEM, (d, e) normalized sample microstructure, and (f, g) hardened (water-quenched) sample microstructure [208].

to overcome challenges and ensure the quality and reliability of the manufactured parts.

Post-processing treatments are critical for addressing residual stresses, improving mechanical properties, and enhancing surface quality in WAAM components. Heat treatment, including stress relief annealing, normalizing, and tempering, is commonly employed to refine microstructure, reduce residual stresses, and improve toughness. However, these processes can be time-consuming and energy-intensive, particularly for large components. Additionally, the selection of appropriate heat treatment parameters is crucial to avoid detrimental effects on mechanical properties.

Surface finishing techniques such as grinding, polishing, and shot peening are employed to enhance dimensional accuracy, surface finish, and fatigue resistance. Grinding and polishing can remove surface irregularities and improve aesthetic appearance but may introduce additional defects if not performed carefully. Shot peening is a more efficient method for inducing compressive residual stresses, improving fatigue life, and enhancing corrosion resistance. However, the equipment and expertise required for shot peening can increase costs.

Other post-processing techniques, such as laser peening and hot isostatic pressing (HIP), offer additional benefits. Laser peening can introduce compressive residual stresses to improve fatigue life, while HIP can consolidate porosity and refine microstructure. However, these techniques are generally more expensive and require specialized equipment. The choice of post-processing technique depends on factors such as component geometry, material type, desired properties, and cost constraints. A comprehensive evaluation considering effectiveness, cost,

and applicability to various steel alloys is essential for optimizing component performance and providing practical guidance to industry practitioners.

4. Effect of defects minimizing methods on properties of steel parts fabricated by WAAM

Process parameters significantly influence defect formation in WAAM. WFS and TS are critical factors. A 10 % increase in WFS can lead to a 15 % increase in porosity [134], while a 20 % increase in TS can decrease porosity by 66 % [1], also, the both UTS and average hardness increased by 10 % highlighting the complex interplay between these parameters. Arc current also influences porosity and lack of fusion. Optimizing these parameters is crucial for minimizing defects and achieving desired component quality. Understanding these relationships is essential for developing robust process control strategies.

Fig. 9 provides a comprehensive view of the microstructure and mechanical properties of 420 martensitic stainless-steel components produced using the WAAM process under varying conditions [207]. The microstructure analysis of the as- fabricated sample reveals intriguing features, including a relatively limited volume fraction of retained austenite and inter-dendritic δ -ferrite embedded within the un-tempered martensitic matrix. Additionally, the as- fabricated sample exhibits a modest volume percentage of retained austenite.

Upon subjecting the material to an austenitizing treatment at 1150°C, a remarkable increase in microhardness is observed, reaching a value of (670 ± 4 HV). This elevation signifies the achievement of a fully

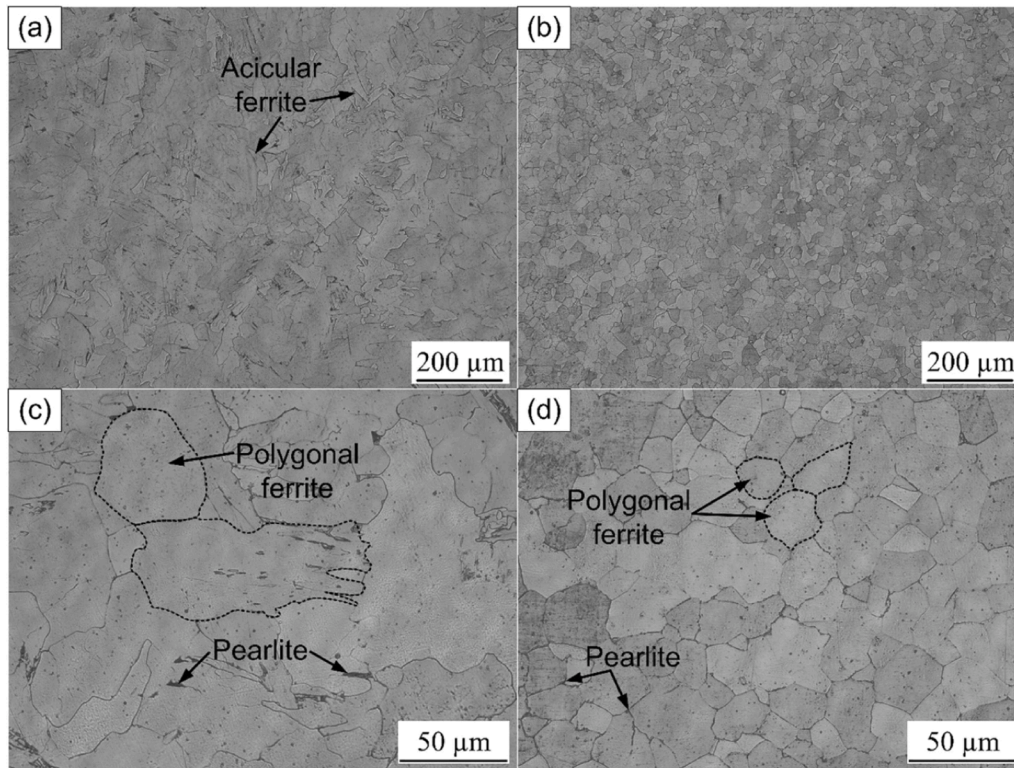


Fig. 11. Optical micrographs of the printed WAAM ER70S-6 alloy, taken at various magnifications (a) and (c) for the final construction; (b) and (d) for the intermediate build [153].

martensitic microstructure characterized by a higher carbon content after the quenching process. In comparison, the microhardness of the as-printed sample stands at $(550 \pm 12 \text{ HV})$.

Remarkably, the tensile strength of the material subjected to the 1150°C austenitizing treatment experiences a significant boost, reaching a value of (UTS of $1903 \pm 12 \text{ MPa}$). This represents a substantial enhancement over the tensile strength of the as-fabricated sample, which records (UTS of $1151 \pm 9 \text{ MPa}$). However, this increase in strength comes at the expense of reduced ductility, evident in the limited elongation of approximately $\sim 1.7\%$ observed in the 1150°C -treated sample.

Subsequent tempering treatments result in a decrease in microhardness values. Notably, the microhardness values observed after tempering at different temperatures—T600, T500, T400, T300, and T200—stand at $(300 \pm 1 \text{ HV})$, $(490 \pm 7 \text{ HV})$, $(550 \pm 7 \text{ HV})$, $(440 \pm 4 \text{ HV})$, and $(460 \pm 3 \text{ HV})$, respectively. These values are in contrast to the microhardness of $(670 \pm 4 \text{ HV})$ achieved through the A1150 austenitizing treatment.

Upon a thorough analysis, the researchers identify the optimal tempering temperature as T400, which provides a well-balanced set of mechanical properties. Specifically, the T400 tempering treatment yields an elongation of $(11.8 \pm 1\%)$, a UTS of $(1442 \pm 5 \text{ MPa})$, and a microhardness value of $(550 \pm 7 \text{ HV})$. Notably, alternative tempering temperatures either result in inadequate strength or contribute to brittleness within the material. This detailed investigation underscores the significance of tempering temperature in tailoring the mechanical characteristics of WAAM-produced 420 martensitic stainless-steel components.

WAAM-fabricated 420 martensitic stainless-steel parts show enhanced strength post-austenitization at 1150°C , albeit with reduced ductility. Subsequent tempering, especially at T400, yields a balanced mechanical profile. Optimal properties include 11.8% elongation, 1442 MPa UTS, and 550 HV microhardness. Tempering at other temperatures results in inadequate strength or brittleness. These findings highlight the

importance of precise processing control to tailor desired attributes of WAAM steel components.

To shed light on the influence of heat treatment on the microstructure and mechanical properties of WAAM-produced steel components, Vahedi Nemani et al. [208] conducted an investigation. This study focused on ER70S-6 steel components and involved the application of two distinct heat treatment cycles - hardening and normalizing. Fig. 10 illustrates the as-printed, normalized, and hardened sample's microstructure. The normalizing heat treatment played a crucial role in eliminating unstable constituents within the material, ultimately facilitating the development of a uniform ferritic/pearlitic microstructure. On the other hand, the hardening heat treatment induced a combination of distinct microstructural phases, leading to a notable enhancement in both hardness and overall strength of the material. The primary microstructure in the as-printed WAAM-ER70S-6 component consisted of polygonal ferrite grains. A smaller volume fraction of lamellar pearlite was present within these grains and along melt pool boundaries. Additionally, a heat-affected zone with coarser polygonal ferrite grains formed adjacent to each deposited track due to the layer-by-layer deposition process. Utilizing the GTAW technique on the same material reveals distinct microstructural shifts based on the build direction [153]. The upper layers displayed a notable blend of acicular and polygonal ferrite in Fig. 11, showing minimal secondary pearlite phase and no pore defects. This transformation from polygonal to acicular ferrite was attributed to a faster cooling rate at the final construction surface. Conversely, the middle build wall exhibited a small amount of pearlite phase in a lamellar arrangement along primary ferrite grain boundaries, set within a matrix of fine polygonal ferrite that's characteristic of this welding method. Following normalizing treatment, meta-stable elements (AF and B) were eliminated from the microstructure, leading to a more uniform HAZ with a ferritic/pearlitic microstructure at the melt pool center. Conversely, the hardening treatment changed the as-printed microstructure into AF, B, and P phases.

Microhardness distribution varied across zones for both as-

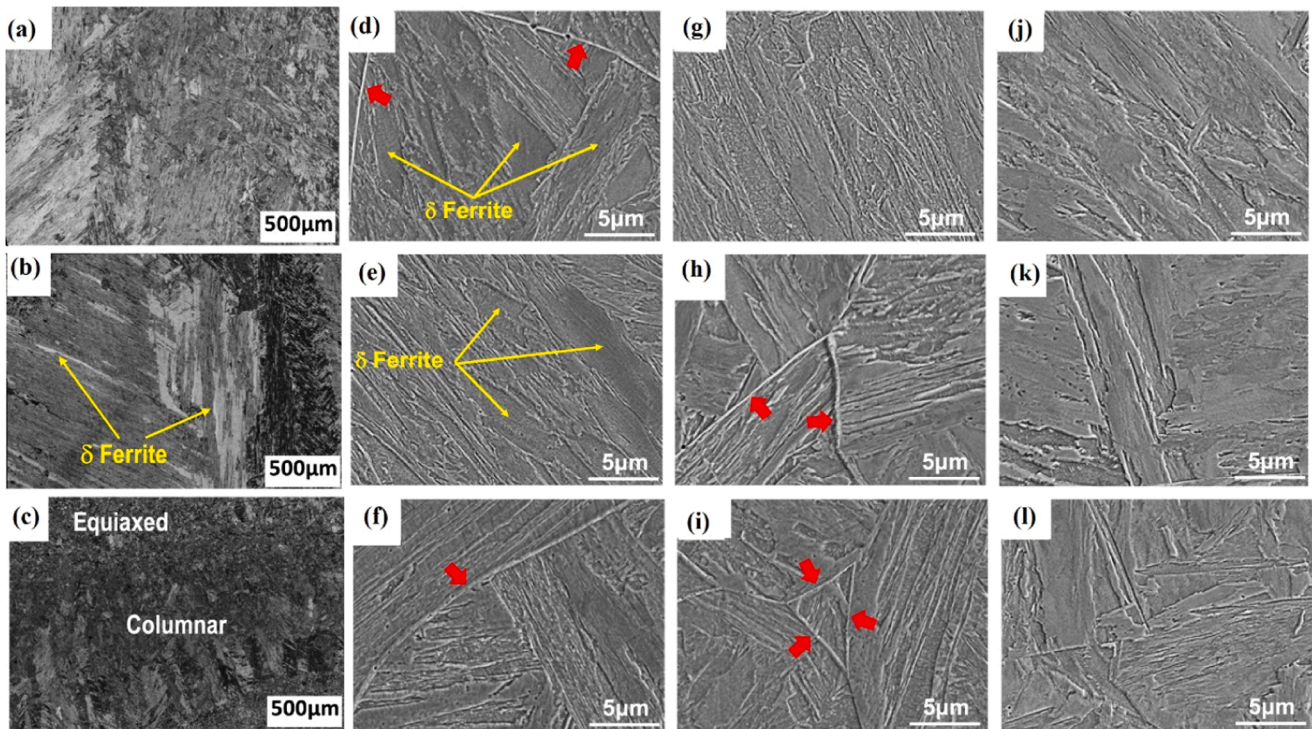


Fig. 12. (a, b, and c) Optical microstructure of the as-printed samples at top, middle, and bottom areas respectively, (d, e, and f) optical microstructure of homogenized at 1200°C for 1h at top, middle, and bottom areas respectively, (g, h, and i) optical microstructure of homogenized at 1200°C for 2h at top, middle, and bottom areas respectively, and (j, k, and l) optical microstructure of homogenized at 1200°C for 3h at top, middle, and bottom areas respectively [209].

fabricated and heat-treated samples. The as-printed sample had a microhardness of 160 ± 7 HV, while the normalized sample exhibited a microhardness of 154 ± 1 HV, similar to the as-printed melt pool center. In contrast, the hardened sample displayed significantly higher microhardness (260 ± 3 HV) due to the presence of AF, B, and P phases.

Tensile strengths for vertical and horizontal orientations were approximately 500 MPa for the as-printed sample, with distinct ductility anisotropy (12 ± 3 % vertical, 35 ± 2 % horizontal). After hardening heat treatment, tensile strengths increased to 624 ± 13 MPa (horizontal) and 640 ± 14 MPa (vertical), accompanied by a slight reduction in ductility. Normalized samples exhibited slightly lower tensile strength (~ 465 MPa) and a minor decrease in microhardness compared to the as-

printed sample, with minimal variation in elongation— 29 ± 2 % in the vertical and 34 ± 3 % in the horizontal orientations.

The heat treatment effectively alters the microstructure and mechanical properties of WAAM-produced steel components, offering insights into potential strategies for tailoring material characteristics according to specific application requirements.

To delve into the impact of heat treatment on WAAM-produced steel components, Li et al. [209] conducted a study focusing on P91 steel samples. Through their investigation, significant improvements were observed in both hardness and microstructure following homogenization at 1200°C (Fig. 12). The transformation of δ -ferrite to lath martensite led to heightened hardness and increased strength compared

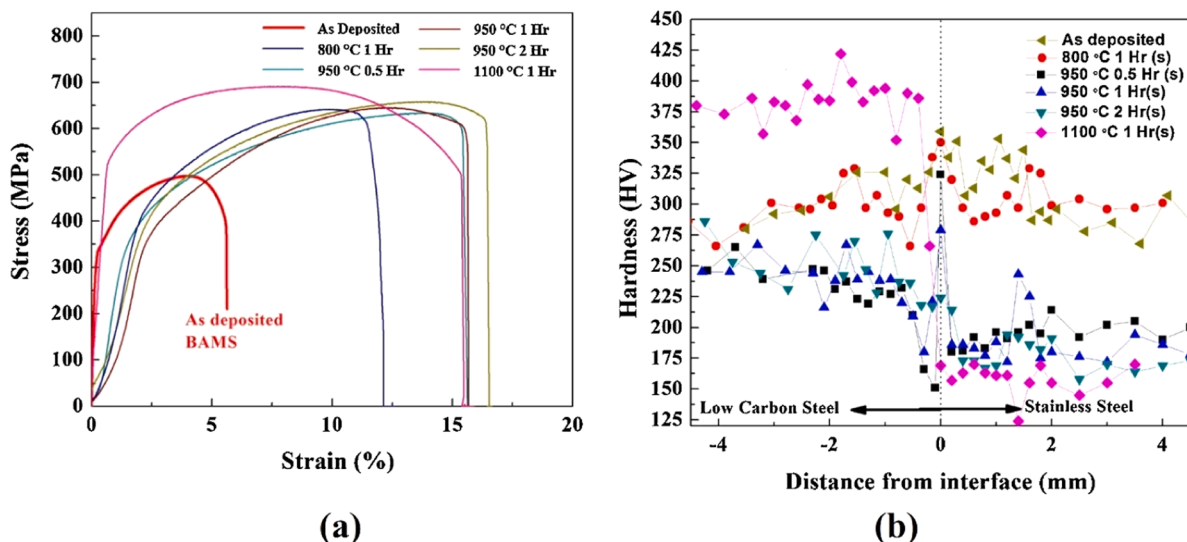


Fig. 13. (a) Stress-strain curve and (b) Microhardness of different heat treatments [210].

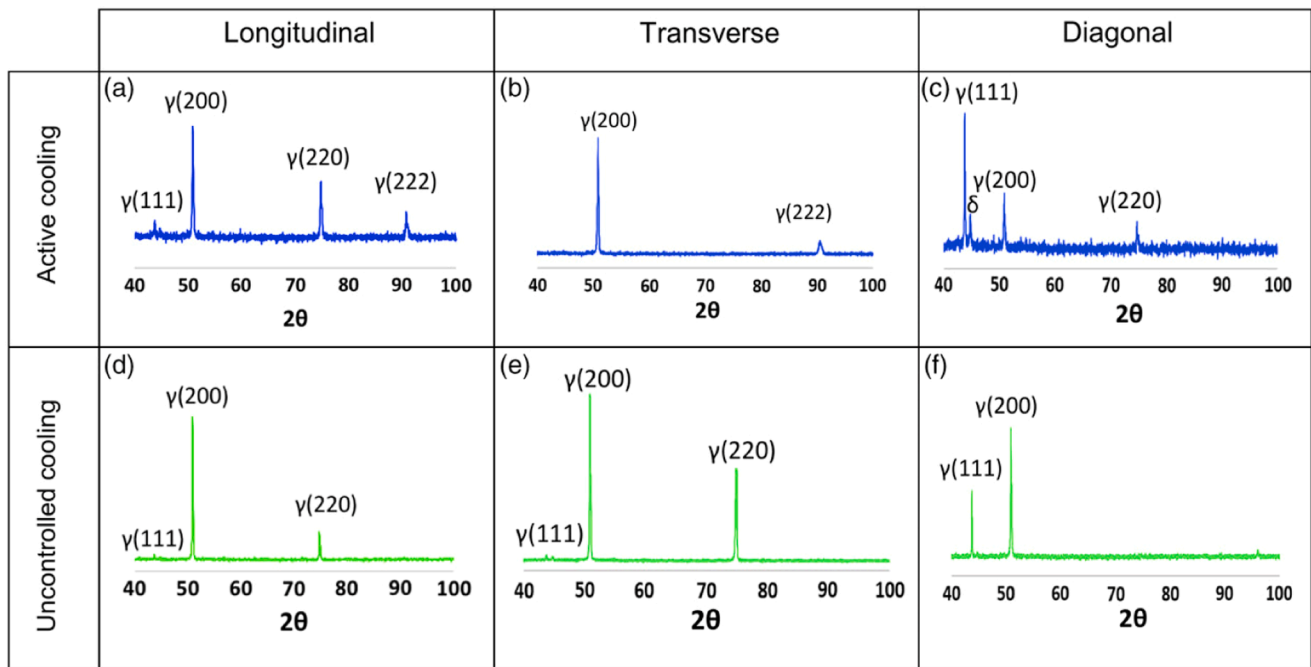


Fig. 14. X-ray diffraction (XRD) of both cooled and uncooled samples [211].

to the as-printed sample. Subsequent aging at 760°C, however, induced a reduction in hardness due to microstructural evolution, notably the precipitation of M23C6, which resulted in material softening. Nonetheless, the heat-treated sample showed improved ductility and tensile strength, rendering it a viable choice for specific applications. Conversely, the as-printed sample displayed exceptional ultimate tensile strength and yield strength, making it suitable for applications requiring elevated strength.

Ahsan et al. [210] explored heat treatment effects on BAMS samples, encompassing austenitic stainless steel and low-carbon steel. Their investigation highlighted a specific heat treatment condition – 950°C for 1 hour – yielding substantial enhancements in mechanical properties (Fig. 13). Microstructural changes, including ferrite-to-ferrite-bainite and austenite transformation, played a pivotal role in augmenting elongation, ultimate tensile strength, and yield strength. These findings underscore the strategic utilization of heat treatment to tailor the properties of BAMS components, aligning with specific requirements.

These studies underscore the pivotal role of heat treatment in shaping the microstructure and mechanical properties of WAAM components. Well-optimized heat treatment processes hold the potential to elevate performance and mechanical traits, positioning WAAM as a versatile and promising manufacturing method across diverse applications. Armed with an understanding of heat treatment’s influence,

designers and engineers can judiciously select appropriate conditions to achieve desired material attributes, thus maximizing the performance of WAAM-produced components.

Investigations into the influence of various inter-pass cooling methods on the microstructure and mechanical properties of steel samples produced using the wire WAAM process have been extensively studied [146,164,211]. These thorough analyses consistently reveal that there are negligible discrepancies observed in both the microstructural characteristics and mechanical responses between samples subjected to different cooling techniques.

Detailed X-ray diffraction (XRD) assessments confirm that both the cooled and uncooled samples exhibit congruent phase compositions, with major peaks corresponding to γ -austenite and δ -ferrite. Additionally, the XRD analysis elucidates that the predominant peak of γ -austenite in the diagonal (D) sample corresponds to (111), whereas for the transverse (T) and longitudinal (L) samples, it corresponds to (200) for both cooled and uncooled specimens as shown in Fig. 14.

Focusing specifically on the diagonal sample (D), the outcomes of tensile tests reveal that the ultimate tensile strength (UTS) of the cooled samples is reported as 608 ± 77 MPa, while the UTS of the uncooled samples is 602 ± 41 MPa [211]. These implies that the cooling techniques employed during inter-pass intervals have limited influence on the tensile response of components manufactured through the WAAM

Table 3
Rolling Effect on Mechanical properties.

Authors & Ref.	Filler Wire	Rolling load	Mechanical properties					
			As-deposited			Rolled		
			UTS (MPa)	%Elongation	Hardness (HV)	UTS (MPa)	%Elongation	Hardness (HV)
[186]	Bainite steel	5 kN	1258	11.0	Not-mentioned	1275	17.4	Not-mentioned
[187]	ER70S-6	50 kN	402 ± 2.0	28 ± 1	186 ± 2.0	546 ± 3.0	32 ± 2	219 ± 1.5
		75 kN				552 ± 1.0	25 ± 2	225 ± 1
		160 kN				600 ± 3.0	22 ± 2	233 ± 1.5
[213]	Maraging steel	50 kN	1118 ± 94	11.7 ± 0.8	322	1138 ± 118	9.2 ± 4.5	351
		75 kN				1152 ± 127	9.9 ± 3.7	406
[212]	ER70s-6	136 N	480 MPa	37.6	Not-mentioned	530 MPa	38.2	Not-mentioned
[185]	ER70S-6	25 kN	Not-mentioned		185	Not-mentioned		195
		50 kN						226
		75 kN						260

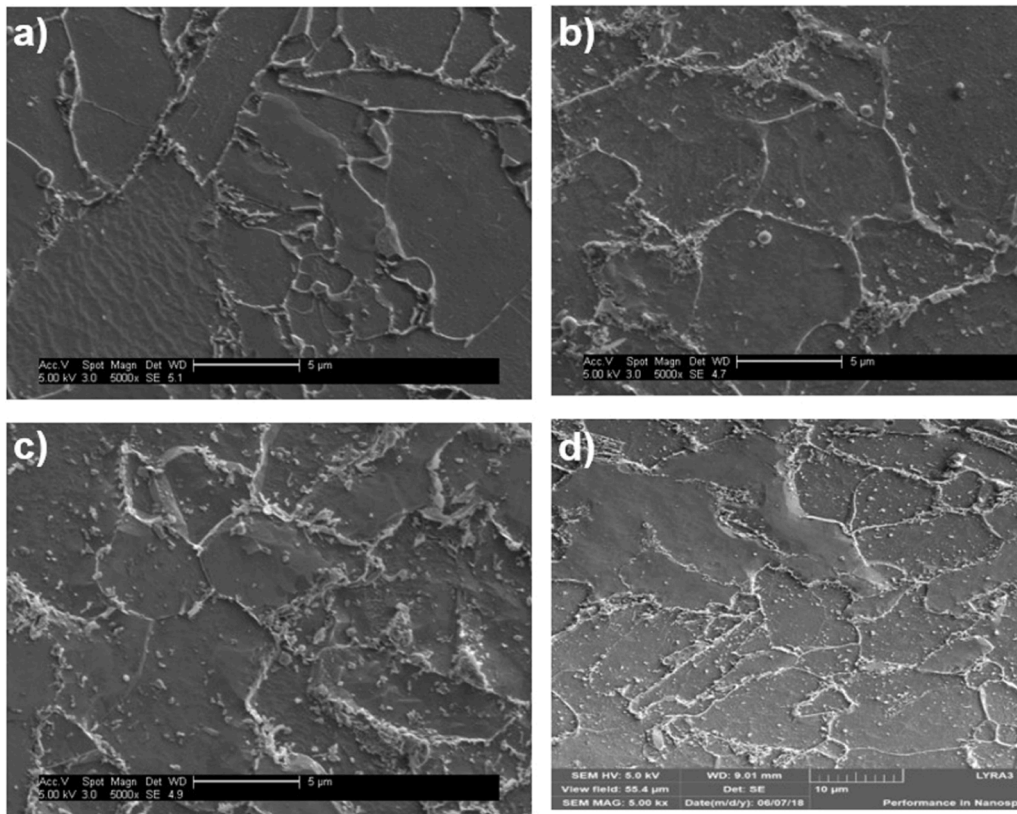


Fig. 15. SEM images (a) as-deposited (b) at 50 kN rolling load (c) at 75 kN rolling load (d) at 160 kN rolling load [187].

process.

The collective evidence from these investigations, along with XRD analysis and tensile test results, robustly indicate that the adoption of different inter-pass cooling methods during the wire WAAM process does not lead to significant deviations in the microstructural attributes and mechanical properties of steel samples. This further suggests that the specific cooling methodologies studied in these analyses exert only minimal impact on the overall tensile behavior of components manufactured using the wire WAAM technique.

Numerous scientific investigations [185–187,212,213] have provided compelling evidence regarding the profound impact of cold working rolling on the mechanical properties of components produced by WAAM, as highlighted comprehensively in Table 3.

In an insightful study [187], distinct rolling loads (50 kN, 75 kN, and 160 kN) were meticulously examined to discern their influence on hardness. The outcomes revealed a distinct trend wherein higher rolling

loads, exemplified by the 160 kN condition, induced a substantial elevation in hardness levels, yielding a prominent 25.26 % enhancement (233 ± 1.5 HV) compared to the as-deposited counterpart (186 ± 2.0 HV). This marked elevation in hardness is attributed to the phenomenon of work-hardening, arising from intensified dislocation density resulting from the augmented rolling load. Furthermore, the microstructural analysis of the rolled samples unveiled a discernible reduction in the average size of elongated grains ($8.6 \mu\text{m}$ for the 160 kN sample in contrast to $14.5 \mu\text{m}$ for the as-deposited specimen) as shown in Fig. 15. This microstructural refinement is accredited to the accumulation of dislocations at the lath martensite interface, contributing to the observed enhancement in hardness [214,215].

Evidently demonstrated in Fig. 15, the pivotal role of rolling in mitigating SW holds profound implications for the mechanical performance of WAAM deposits. Notably, the application of a rolling load of 160 kN yielded a remarkable 55.5 % reduction in SW, coinciding with a

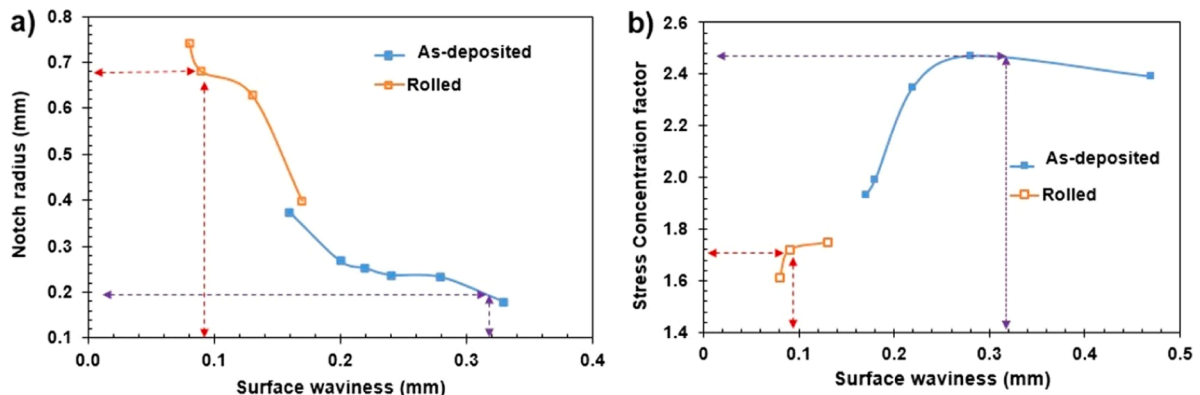


Fig. 16. (a) Effect of notch radius on SW (b) Effect of SCF on SW in rolled and as-deposited conditions [187].

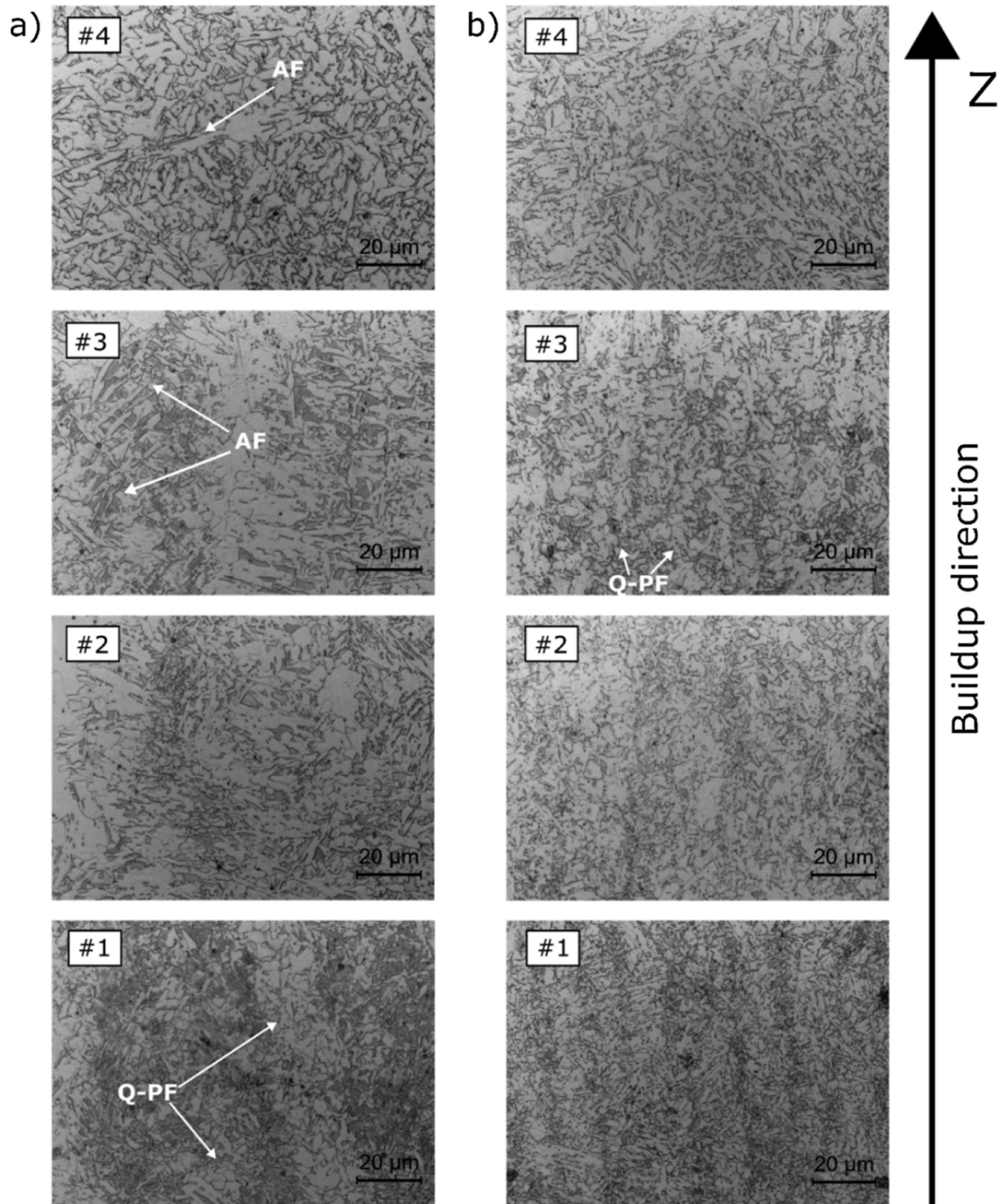


Fig. 17. OM image of samples (a) P1 and (b) P2 along building direction [216].

substantial 49.25 % augmentation in UTS. Equally noteworthy, a rolling load of 75 kN led to a discernible 27 % reduction in SW, accompanied by a substantial 37.5 % increase in UTS.

The incorporation of cold working rolling technique shows significant potential in enhancing mechanical properties. Table 3 illustrates that elevated rolling loads correlate with increased microhardness and average UTS, attributed to heightened dislocation density and induced work-hardening. Moreover, rolling implementation yields smaller average grain sizes compared to as-deposited samples, further amplifying mechanical enhancements.

The strategic integration of cold working rolling into the WAAM

process emerges as a promising approach, clearly demonstrating the potential to elevate mechanical properties such as hardness, UTS, and YS, thereby enhancing the overall performance and quality of produced WAAM components. Fig 16

The manipulation of welding parameters, such as WFS and TS, yields significant influence over HI, as denoted by Eq. (1). This, in turn, imparts a noticeable impact on the mechanical characteristics of the deposited specimens. In situations where HI is elevated, there is a corresponding rise in heat accumulation. Consequently, hardness values and strength diminish due to the absence of bainite formation [216]. However, this elevation contributes to enhanced ductility, attributed to an increased

Table 4
HI effect on mechanical properties.

Authors & Ref.	Filler Wire	Optimizing methods and parameters.	Mechanical properties		
			UTS (MPa)	% Elongation	Hardness (HV)
Yildiz et al. [179]	ER120S-G	Controlling WFS/TS parameter or HI			
		Single-bead low-heat (SBLH) / WFS/TS=10 / HI= 339 J/mm	986 ± 38	16.6 ± 0.8	330 ± 19
		Single-bead high-heat (SBHH) / WFS/TS=20 / HI= 559 J/mm	955 ± 49	20.1 ± 2.6	318 ± 18
Aldalur et al [218]	ER70S-6	Multiple-bead oscillation (MBO) / WFS/TS=10 / HI= 361 J/mm	994 ± 6	24.2 ± 0.8	295 ± 11
		Controlling the in-volume HI HI _{3D}			
		The overlapping deposition strategy HI _{3D} = 48.67 J/mm ³	H 498 ± 8.8 V 501 ± 2.87	H 36 ± 3.5 V 32 ± 1.1	Top 163 Centre 146 Bottom 144
		The oscillating deposition strategies HI _{3D} = 67.17 J/mm ³	H 478 ± 6.41 V 474 ± 0.94	H 38 ± 2.6 V 36 ± 2.2	Top 154 Centre 136 Bottom 135
(Rodrigues et al. [216])	ER110S-G	Depositing at different TS			
		Sample P1 / TS= 3.9 mm/s / HI= 511 J/mm	H 750 V 795	H 19.6 V 25.6	229–320
Wu et al. [217]	316L stainless steel	Sample P2 / TS= 9 mm/s / HI= 221 J/mm	H 700 V 749	H 17.1 V 19.9	247–311
		Different arc modes			
		Speed cold (S-C) welding processes sample	578.76 ± 30.458	Not-mentioned	174.9
		Speed arc (S-A)welding processes sample	607.2 ± 44.87	Not-mentioned	177.4

formation of ferrite content [179].

On the contrary, the augmentation of TS leads to a reduction in HI, transitioning from 511 J/mm at 3.9 mm/s to 221 J/mm at 9 mm/s, which also leads to an accelerated solidification rate. This phenomenon results in a decrease in equiaxed grain size and a decline in volume fraction, as detailed by Rodrigues et al. [216]. The iterative process of reheating and thermal accumulation induces the development of coarser grain size along the build direction. As the material cools from high temperatures, the transition from austenite to ferrite occurs. This transformation involves the creation of allotriomorphic ferrite at the boundaries of the earlier austenite grains. Subsequently, nucleation of side-plate ferrite may start at interfaces between austenite and ferrite,

extending into non-transformed austenite grains. Various forms of ferrite formation, including allotriomorphic, side-plate, acicular, and bainitic ferrite, are influenced by factors such as material microstructure, specific inclusions, cooling rate, and local thermal conditions as depicted in Fig. 17.

Consequently, this culminates in a decrease in hardness from 320 to 229 HV for sample P1 and from 311 to 247 HV for sample P2, as indicated in Table 4. Particularly, the initial deposited layers exhibit improved hardness owing to rapid cooling facilitated by efficient heat dissipation from the substrate [217]. This transformative effect is visually depicted in Fig. 18, wherein the grain size transitions from coarser in the upper and middle sections to comparatively finer grains in the lower regions of the sample.

As per Table 4, sample S-C exhibits a recorded tensile strength of 578.76 ± 30.458 MPa, while sample S-A achieves a tensile strength of 607.2 ± 44.87 MPa. Although the tensile properties of sample S-A are commendable, a significant anisotropy of up to 13.3 percent is evident, highlighting a discernible divergence in properties across different orientations.

The manipulation of welding parameters in WAAM has a substantial impact on material properties. Varying welding parameters, like WFS and TS, profoundly affect HI, influencing material properties. Increased HI reduces hardness and strength, favoring ductility via higher ferrite content. Enhanced TS yields finer grain and reduced hardness. This underscores the crucial role of precise parameter control to meet the requirements of diverse applications.

5. Developments and innovations

The evolution of WAAM is intrinsically linked to advancements in materials science. The development of novel alloys specifically engineered for additive manufacturing has expanded the application horizons of this technology. These alloys often exhibit superior properties such as enhanced strength-to-weight ratios, improved corrosion resistance, and tailored thermal expansion coefficients. For instance, high-strength low-alloy (HSLA) steels with optimized compositions have shown promise in WAAM for structural applications. Additionally, the incorporation of microalloying elements can refine microstructure and enhance mechanical properties [219].

Beyond alloy development, the quality of feedstock materials has also undergone significant improvements. The availability of high-purity metal wires with consistent chemical composition and reduced impurity levels has contributed to enhanced process stability and component quality. Moreover, the development of clad wires, incorporating multiple materials within a single wire, offers opportunities for creating functionally graded materials and complex components with varying properties. These advancements in materials science are essential for realizing the full potential of WAAM and expanding its industrial applications.

Significant strides have been made in refining WAAM processes to enhance efficiency, quality, and productivity. The development of hybrid processes, combining WAAM with other additive or subtractive techniques such as laser or powder bed fusion, has expanded the fabrication envelope, enabling the creation of complex components with tailored properties. For instance, laser-assisted WAAM can improve melt pool dynamics, reduce porosity, and enhance metallurgical bonding.

Automation and robotics have revolutionized WAAM operations. The integration of industrial robots with advanced motion control systems has enabled precise and rapid deposition of materials, increased production rates and reducing labor costs. Additionally, the use of collaborative robots (cobots) has enhanced human-machine interaction, facilitating flexible and adaptable manufacturing processes [220].

In-situ monitoring and control systems have emerged as critical components of modern WAAM systems. Sensors for temperature, melt pool dimensions, and acoustic emissions provide real-time process feedback, enabling adjustments to process parameters to prevent defects

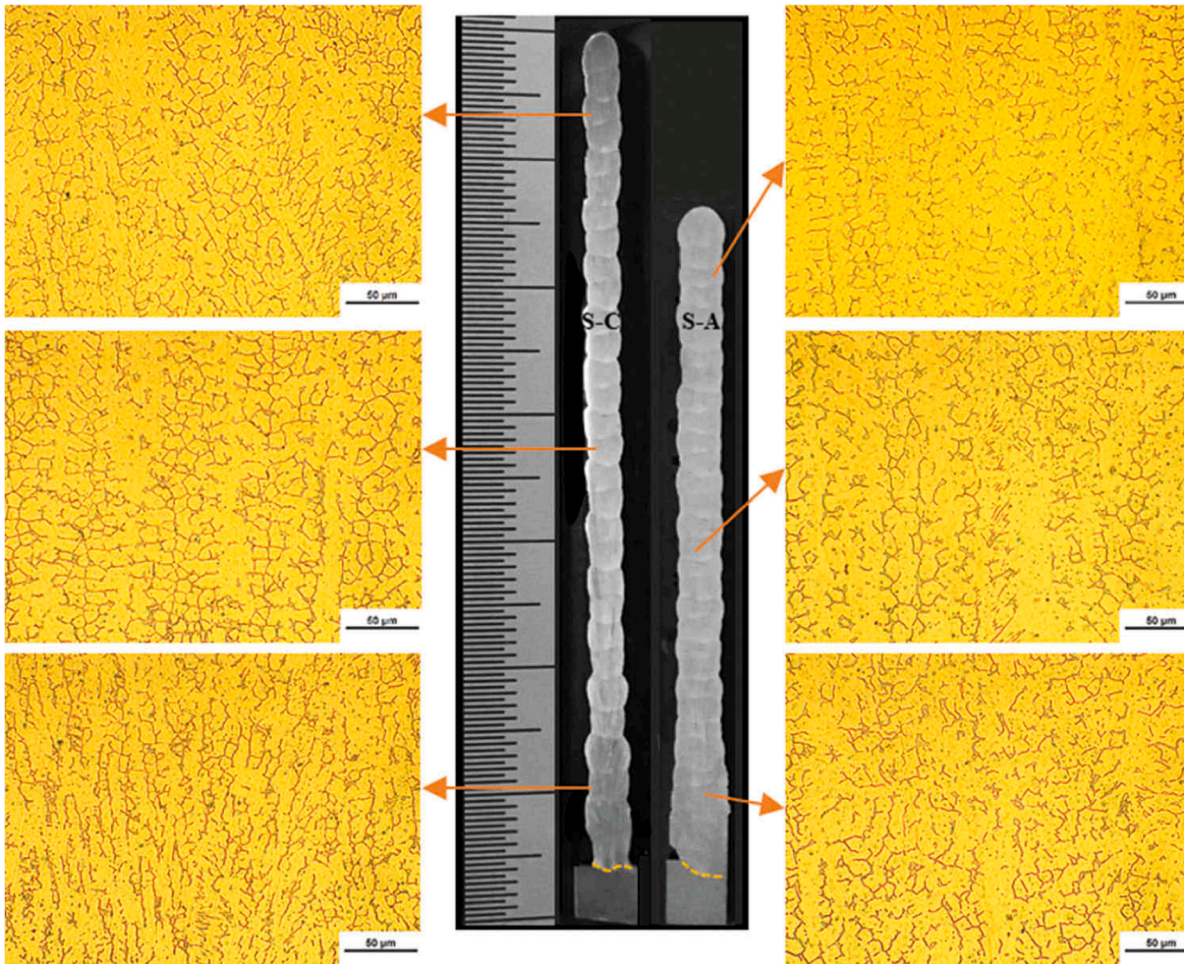


Fig. 18. S-C and S-A samples' vertical cross-section micrographs and microstructures [217].



Fig. 19. Various WAAM applications.

and maintain consistent quality. Closed-loop control systems can automatically correct deviations from desired process conditions, ensuring optimal performance. These process innovations collectively contribute

to the maturation of WAAM as a viable manufacturing technology.

The integration of advanced software and modeling tools has significantly contributed to the progress of WAAM. Sophisticated

simulation software enables researchers and engineers to virtually predict process behavior, optimize parameters, and minimize defects. These tools can simulate thermal gradients, fluid flow, and solidification processes, providing valuable insights into the underlying mechanisms of WAAM. Additionally, the development of design software specifically tailored for WAAM-specific geometries has facilitated the creation of optimized components. These software packages consider factors such as build orientation, support structures, and material distribution to ensure manufacturability and part performance. By leveraging these software advancements, the WAAM industry can enhance design efficiency, reduce prototyping costs, and accelerate product development cycles [70,221].

6. Applications and case studies

WAAM has demonstrated significant potential across various sectors, with the steel industry being a prime beneficiary as indicated in Fig. 19. From large-scale infrastructure to complex components, WAAM has shown its versatility. In particular, the energy sector has leveraged WAAM for the fabrication of turbine components, pressure vessels, and repair of critical equipment [86]. The transportation industry has explored its application in producing automotive and aerospace parts, capitalizing on its ability to create complex geometries. Additionally, the construction industry has shown interest in using WAAM for the production of steel structures and components, offering potential benefits in terms of construction speed and material efficiency [222].

Several case studies highlight the successful application of WAAM in the energy sector. For instance, researchers have developed large-scale turbine components using WAAM, demonstrating the technology's potential for reducing manufacturing costs and lead times. Repair of damaged turbine blades through WAAM has also been explored, offering a cost-effective alternative to traditional repair methods. The automotive industry has investigated WAAM for producing complex components such as chassis parts and engine blocks. Aerospace manufacturers have explored the use of WAAM for fabricating large-scale structural components, taking advantage of the technology's ability to create complex geometries with internal channels for cooling or wiring.

WAAM has shown promise in the construction sector for producing customized steel reinforcement bars, bridge components, and building facades. Case studies have demonstrated the potential for rapid construction and reduced material waste through the use of WAAM.

7. Conclusions and future work

7.1. Conclusions

Wire Arc Additive Manufacturing (WAAM) holds significant promise for producing steel components, offering advantages in design flexibility, rapid prototyping, and material efficiency. However, challenges such as porosity, lack of fusion, and residual stresses persist, necessitating careful process control and post-process treatments. Achieving optimal component quality requires a comprehensive understanding of heat transfer, material behavior, and defect formation mechanisms. Recent advancements, including hybrid processes, in-situ monitoring, and advanced materials, have shown potential for addressing these challenges. To fully realize WAAM's potential, continued research and development are crucial to optimize process parameters, enhance microstructure control, and expand the range of producible components.

7.2. Future work

The future of WAAM in steel manufacturing holds immense promise. As research and development continue, we can anticipate significant advancements in materials, processes, and applications. Emerging technologies such as artificial intelligence and machine learning will play a pivotal role in optimizing process parameters, predicting

component properties, and accelerating product development. Furthermore, the integration of WAAM with other manufacturing processes, such as forging and casting, will create hybrid approaches with enhanced capabilities. The potential for producing large-scale, complex steel structures with tailored properties through WAAM is particularly exciting. As the technology matures, it is expected to become increasingly integrated into the manufacturing landscape, contributing to sustainable and efficient production processes.

Funding

Not applicable.

Availability of data and material

Up on request.

Code availability

Not applicable.

Ethics approval

Not applicable.

Consent to participate

Not applicable.

Consent for publication

Not applicable.

CRediT authorship contribution statement

Mohamed Dekis: Writing – original draft, Methodology, Investigation, Conceptualization. **Mahmoud Tawfik:** Investigation, Conceptualization. **Mohamed Egiza:** Writing – review & editing, Methodology, Conceptualization. **Montaser Dewidar:** Writing – review & editing, Supervision.

Declaration of competing interest

The authors declare that they have no known competing financial interests or personal relationships that could have appeared to influence the work reported in this paper.

Acknowledgment

The authors gratefully acknowledge the support from the Faculty of Engineering at Kafrelsheikh University for this work. Additionally, they extend their heartfelt thanks to the anonymous reviewers for their valuable efforts and insightful comments.

Data availability

No data was used for the research described in the article.

References

- [1] M. Dekis, M. Tawfik, M. Egiza, M. Dewidar, Unveiling the characteristics of ER70S-6 low carbon steel alloy produced by wire arc additive manufacturing at different travel speeds, *Met. Mater. Int.* (2024), <https://doi.org/10.1007/s12540-024-01766-x>.
- [2] J.P.M. Pragana, R.F.V. Sampaio, I.M.F. Bragança, C.M.A. Silva, P.A.F. Martins, Hybrid metal additive manufacturing: A state-of-the-art review, *Adv. Ind. Manuf. Eng.* 2 (2021) 100032, <https://doi.org/10.1016/j.aime.2021.100032>.

- [3] R. Agarwal, V. Gupta, J.J.J.o.t.B.S.o.M.S. Singh, Engineering, additive manufacturing-based design approaches and challenges for orthopaedic bone screws: a state-of-the-art review, *J. Brazil. Soc. Mech. Sci. Eng.* 44 (1) (2022) 1–25, <https://doi.org/10.1007/s40430-021-03331-8>.
- [4] M.S. Kumar, C.-H. Yang, V. Aravinthan, A.A. Adediran, S.R. Begum, M. Vasumathi, T.C. Jen, Influence of low heat input by CMT powered WAAM on attaining the microstructural and mechanical homogeneity of printed 304 SS cylindrical component, *Results. Eng.* 21 (2024) 101846, <https://doi.org/10.1016/j.rineng.2024.101846>.
- [5] W.E. Frazier, Metal Additive Manufacturing: A review, *J. Mater. Eng. Perform.* 23 (6) (2014) 1917–1928, <https://doi.org/10.1007/s11665-014-0958-z>.
- [6] B. Baufeld, O.V.d. Biest, R. Gault, Additive manufacturing of Ti-6Al-4V components by shaped metal deposition: microstructure and mechanical properties, *Mater. Des.* 31 (2010) S106–S111, <https://doi.org/10.1016/j.matdes.2009.11.032>.
- [7] Z.Q. Yin, G.J. Zhang, H.H. Zhao, L. Wu, Rapid manufacturing and remanufacturing system based on robotic GMAW, *Adv. Mat. Res.* 156–157 (2011) 1626–1629, <https://doi.org/10.4028/www.scientific.net/AMR.156-157.1626>.
- [8] A. Busachi, J. Erkoyuncu, P. Colegrove, F. Martina, C. Watts, R. Drake, A review of additive manufacturing technology and cost estimation techniques for the defence sector, *CIRP. J. Manuf. Sci. Technol.* 19 (2017) 117–128, <https://doi.org/10.1016/j.cirpj.2017.07.001>.
- [9] C. Yin, J. Shen, S. Hu, Z. Zhang, Microstructure and mechanical properties of AZ91 magnesium alloy fabricated by multi-layer and multi-pass CMT based WAAM technique, *Results. Eng.* 18 (2023) 101065, <https://doi.org/10.1016/j.rineng.2023.101065>.
- [10] H.T. Serindağ, G.J.J.o.M.E. Çam, Performance, characterizations of microstructure and properties of dissimilar AISI 316L/9Ni low-alloy cryogenic steel joints fabricated by gas tungsten arc welding, *J. Mater. Eng. Perform.* 32 (15) (2022) 1–11, <https://doi.org/10.1007/s11665-022-07601-x>.
- [11] A. Queguineur, G. Rückert, F. Cortial, J.Y. Hascoët, Evaluation of wire arc additive manufacturing for large-sized components in naval applications, *Weld. World* 62 (2) (2018) 259–266, <https://doi.org/10.1007/s40194-017-0536-8>.
- [12] F. Hejripour, F. Binesh, M. Hebel, D.K. Aidun, Thermal modeling and characterization of wire arc additive manufactured duplex stainless steel, *J. Mater. Process. Technol.* 272 (2019) 58–71, <https://doi.org/10.1016/j.jmatprotec.2019.05.003>.
- [13] P. Dirisu, S. Ganguly, A. Mehmanparast, F. Martina, S. Williams, Analysis of fracture toughness properties of wire + arc additive manufactured high strength low alloy structural steel components, *Mater. Sci. Eng. A* 765 (2019) 138285, <https://doi.org/10.1016/j.msea.2019.138285>.
- [14] A. Taşdemir, S. Nohut, An overview of wire arc additive manufacturing (WAAM) in shipbuilding industry, *Ships Offshore Struct.* 16 (7) (2020) 797–814, <https://doi.org/10.1080/17445302.2020.1786232>.
- [15] S.W. Williams, F. Martina, A.C. Addison, J. Ding, G. Pardal, P. Colegrove, Wire + arc additive manufacturing, *Mater. Sci. Technol.* 32 (7) (2016) 641–647, <https://doi.org/10.1179/1743284715y.00000000073>.
- [16] P. Wang, H. Zhang, H. Zhu, Q. Li, M. Feng, Wire-arc additive manufacturing of AZ31 magnesium alloy fabricated by cold metal transfer heat source: processing, microstructure, and mechanical behavior, *J. Mater. Process. Technol.* 288 (2021) 116895, <https://doi.org/10.1016/j.jmatprotec.2020.116895>.
- [17] S. Singh, S.K. Sharma, D.W. Rathod, A review on process planning strategies and challenges of WAAM, in: *Materials Today: Proceedings*, 2021, <https://doi.org/10.1016/j.matpr.2021.02.632>.
- [18] F. Antunes, L. Santos, C. Capela, J. Ferreira, J. Costa, J. Jesus, P. Prates, Fatigue crack growth in maraging steel obtained by selective laser melting, *9 (20) (2019)*, 4412, [doi:10.3390/app9204412](https://doi.org/10.3390/app9204412).
- [19] D.-S. Nguyen, H.-S. Park, C.-M. Lee, Applying selective laser melting to join Al and Fe: an investigation of dissimilar materials, *9 (15) (2019)*, 3031, [doi:10.3390/app9153031](https://doi.org/10.3390/app9153031).
- [20] Z. Tian, C. Zhang, D. Wang, W. Liu, X. Fang, D. Wellmann, Y. Zhao, Y. Tian, A review on laser powder bed fusion of Inconel 625 nickel-based alloy, *Appl. Sci.* 10 (1) (2020), <https://doi.org/10.3390/app10010081>.
- [21] G. Mohr, S.J. Altenburg, A. Ulbricht, P. Heinrich, D. Baum, C. Maierhofer, K. Hilgenberg, In-situ defect detection in laser powder bed fusion by using thermography and optical tomography—Comparison to computed tomography, *Metals* 10 (1) (2020), <https://doi.org/10.3390/met10010103>.
- [22] R. Gandhi, L. Pagliari, R. Gerosa, F. Concli, Quasi-static and fatigue performance of Ti-6Al-4V triply periodic minimal surface scaffolds manufactured via laser powder bed fusion for hard-tissue engineering, *Results. Eng.* 24 (2024) 103101, <https://doi.org/10.1016/j.rineng.2024.103101>.
- [23] B. Mu, X. Wang, X. Zhang, X. Xiao, Laser direct sintering approach for additive manufacturing in flexible electronic, *Results. Eng.* 13 (2022) 100359, <https://doi.org/10.1016/j.rineng.2022.100359>.
- [24] I.J.A.I. Astm, West Conshohocken, PA, ASTM52900-15 standard terminology for additive manufacturing—General principles—Terminology, 3 (4) (2015), 5.
- [25] P.N. Bellamkonda, M. Dwivedy, R. Addanki, Cold metal transfer technology - A review of recent research developments, *Results. Eng.* 23 (2024) 102423, <https://doi.org/10.1016/j.rineng.2024.102423>.
- [26] J. Montero, P. Vitale, S. Weber, M. Bleckmann, K. Paetzold, Indirect additive manufacturing of resin components using polyvinyl alcohol scaffold moulds, *Proc. CIRP.* 91 (2020) 388–395, <https://doi.org/10.1016/j.procir.2020.02.191>.
- [27] Y. Li, C. Su, J. Zhu, Comprehensive review of wire arc additive manufacturing: hardware system, physical process, monitoring, property characterization, application and future prospects, *Results. Eng.* 13 (2022) 100330, <https://doi.org/10.1016/j.rineng.2021.100330>.
- [28] M.A. León-Cabezas, A. Martínez-García, F.J. Varela-Gandía, Innovative advances in additive manufactured moulds for short plastic injection series, *Procedia Manufacturing*, 13 (2017), 732–737, [doi:10.1016/j.promfg.2017.09.124](https://doi.org/10.1016/j.promfg.2017.09.124).
- [29] S. Mitra, A. Rodríguez de Castro, M. El Mansori, On the rapid manufacturing process of functional 3D printed sand molds, *J. Manuf. Process.* 42 (2019) 202–212, <https://doi.org/10.1016/j.jmapro.2019.04.034>.
- [30] C.R. Cunningham, J.M. Flynn, A. Shokrani, V. Dhokia, S.T. Newman, Invited review article: strategies and processes for high quality wire arc additive manufacturing, *Additive Manufacturing*, 22 (2018), 672–686, [doi:10.1016/j.addma.2018.06.020](https://doi.org/10.1016/j.addma.2018.06.020).
- [31] H.-W. Cho, S.-J. Shin, G.-J. Seo, D.B. Kim, D.-H.J.J.o.M.P.T. Lee, Real-time anomaly detection using convolutional neural network in wire arc additive manufacturing: Molybdenum material, *J. Mater. Process. Technol.* 302 (2022) 117495, <https://doi.org/10.1016/j.jmatprotec.2022.117495>.
- [32] K.S. Derekar, A review of wire arc additive manufacturing and advances in wire arc additive manufacturing of aluminium, *Mater. Sci. Technol.* 34 (8) (2018) 895–916, <https://doi.org/10.1080/02670836.2018.1455012>.
- [33] M. Dinovitzer, X. Chen, J. Laliberte, X. Huang, H. Frei, Effect of wire and arc additive manufacturing (WAAM) process parameters on bead geometry and microstructure, *Addit. Manuf.* 26 (2019) 138–146, <https://doi.org/10.1016/j.addma.2018.12.013>.
- [34] J. Pasco, Z. Lei, C. Aranas Jr., Additive manufacturing in off-site construction: review and future directions, *Buildings* 12 (1) (2022) 53, <https://doi.org/10.3390/buildings12010053>.
- [35] Y. Zhao, J. Xiao, S.J. Chen, Comparison of microstructure and mechanical properties of aluminum components manufactured by CMT, *Mater. Sci. Forum* 898 (2017) 1318–1324, <https://doi.org/10.4028/www.scientific.net/MSF.898.1318>.
- [36] V.H.M. R.N. Rao, M. Maiya, P. Kumar, N. Gupta, K.K. Saxena, V. Vijayan, Effects of arc current and travel speed on the processing of stainless steel via wire arc additive manufacturing (WAAM) process, *J. Adhes. Sci. Technol.* 38 (12) (2024) 2222–2239, <https://doi.org/10.1080/01694243.2023.2289770>.
- [37] F. O'Neill, A. Mehmanparast, A review of additive manufacturing capabilities for potential application in offshore renewable energy structures, *Forces Mech.* 14 (2024) 100255, <https://doi.org/10.1016/j.fnmec.2024.100255>.
- [38] B. Wu, Z. Pan, D. Ding, D. Cuiuri, H. Li, J. Xu, J. Norrish, A review of the wire arc additive manufacturing of metals: properties, defects and quality improvement, *J. Manuf. Process.* 35 (2018) 127–139, <https://doi.org/10.1016/j.jmapro.2018.08.001>.
- [39] A. Caballero, J. Ding, S. Ganguly, S. Williams, Wire + arc additive manufacture of 17-4 PH stainless steel: effect of different processing conditions on microstructure, hardness, and tensile strength, *J. Mater. Process. Technol.* 268 (2019) 54–62, <https://doi.org/10.1016/j.jmatprotec.2019.01.007>.
- [40] C.R. Cunningham, S. Wikshåland, F. Xu, N. Kemakolam, A. Shokrani, V. Dhokia, S.T. Newman, Cost modelling and sensitivity analysis of wire and arc additive manufacturing, *Procedia Manuf.* 11 (2017) 650–657, <https://doi.org/10.1016/j.promfg.2017.07.163>.
- [41] X. Xu, J. Ding, S. Ganguly, C. Diao, S. Williams, Preliminary investigation of building strategies of maraging steel bulk material using wire + arc additive manufacturing, *J. Mater. Eng. Perform.* 28 (2) (2019) 594–600, <https://doi.org/10.1007/s11665-018-3521-5>.
- [42] G.J.M.T.P. Çam, Prospects of producing aluminum parts by wire arc additive manufacturing (WAAM), *Mater. Today Proc.* 62 (2022) 77–85, <https://doi.org/10.1016/j.matpr.2022.02.137>.
- [43] B. Tomar, S. Shiva, T. Nath, A review on wire arc additive manufacturing: processing parameters, defects, quality improvement and recent advances, *Mater. Today Commun.* 31 (2022) 103739, <https://doi.org/10.1016/j.mtcomm.2022.103739>.
- [44] M. Srivastava, S. Rathee, A. Tiwari, M. Dongre, Wire arc additive manufacturing of metals: A review on processes, materials and their behaviour, *Mater. Chem. Phys.* 294 (2023) 126988, <https://doi.org/10.1016/j.matchemphys.2022.126988>.
- [45] D. Chakraborty, T. Tirumala, S. Chitral, B.N. Sahoo, D.V. Kiran, P.A. Kumar, The State of the art for wire arc additive manufacturing process of titanium alloys for aerospace applications, *J. Mater. Eng. Perform.* 31 (8) (2022) 6149–6182, <https://doi.org/10.1007/s11665-022-07128-1>.
- [46] M.M. Tawfik, M.M. Nemat-Alla, M.M. Dewidar, Enhancing the properties of aluminum alloys fabricated using wire + arc additive manufacturing technique - A review, *J. Mater. Res. Technol.* 13 (2021) 754–768, <https://doi.org/10.1016/j.jmrt.2021.04.076>.
- [47] Y. Ali, P. Henckell, J. Hildebrand, J. Reimann, J.P. Bergmann, S. Barnikol-Oettler, Wire arc additive manufacturing of hot work tool steel with CMT process, *J. Mater. Process. Technol.* 269 (2019) 109–116, <https://doi.org/10.1016/j.jmatprotec.2019.01.034>.
- [48] J.Z. Li, M.R. Alkahari, N.A.B. Rosli, R. Hasan, M.N. Sudin, F.R. Ramli, Review of wire arc additive manufacturing for 3D metal printing, *Int. J. Autom. Technol.* 13 (3) (2019) 346–353, <https://doi.org/10.20965/ijat.2019.p0346>.
- [49] W. Jin, C. Zhang, S. Jin, Y. Tian, D. Wellmann, W. Liu, Wire arc additive manufacturing of stainless steels: a review, *Appl. Sci.* 10 (5) (2020), <https://doi.org/10.3390/app10051563>.
- [50] M. Rafieazad, M. Ghaffari, A. Vahedi Nemani, A. Nasiri, Microstructural evolution and mechanical properties of a low-carbon low-alloy steel produced by wire arc additive manufacturing, *Int. J. Adv. Manuf. Technol.* 105 (5) (2019) 2121–2134, <https://doi.org/10.1007/s00170-019-04393-8>.
- [51] A. Vahedi Nemani, M. Ghaffari, A. Nasiri, Comparison of microstructural characteristics and mechanical properties of shipbuilding steel plates fabricated

- by conventional rolling versus wire arc additive manufacturing, *Addit. Manuf.* 32 (2020) 101086, <https://doi.org/10.1016/j.addma.2020.101086>.
- [52] C. Zhang, Z. Li, J. Zhang, H. Tang, H. Wang, Additive manufacturing of magnesium matrix composites: comprehensive review of recent progress and research perspectives, *J. Magnes. Alloys* 11 (2) (2023) 425–461, <https://doi.org/10.1016/j.jma.2023.02.005>.
- [53] M.R. Zahidin, F. Yusof, S.H. Abdul Rashid, S. Mansor, S. Raja, M.F. Jamaludin, Y. H.P. Manurung, M.S. Adenan, N.I. Syahriah Hussein, Research challenges, quality control and monitoring strategy for Wire Arc Additive Manufacturing, *J. Mater. Res. Technol.* 24 (2023) 2769–2794, <https://doi.org/10.1016/j.jmrt.2023.03.200>.
- [54] R.F.V. Sampaio, J.P.M. Praga, I.M.F. Bragança, C.M.A. Silva, C.V. Nielsen, P.A. F. Martins, Modelling of wire-arc additive manufacturing – A review, *Adv. Ind. Manuf. Eng.* 6 (2023), <https://doi.org/10.1016/j.aime.2023.100121>.
- [55] M. Laleh, E. Sadeghi, R.I. Revilla, Q. Chao, N. Haghadi, A.E. Hughes, W. Xu, I. De Graeve, M. Qian, I. Gibson, M.Y. Tan, Heat treatment for metal additive manufacturing, *Prog. Mater. Sci.* 133 (2023), <https://doi.org/10.1016/j.pmatsci.2022.101051>.
- [56] L. Gardner, Metal additive manufacturing in structural engineering – review, advances, opportunities and outlook, *Structures* 47 (2023) 2178–2193, <https://doi.org/10.1016/j.istruc.2022.12.039>.
- [57] D. Zhang, A. Liu, B. Yin, P. Wen, Additive manufacturing of duplex stainless steels - A critical review, *J. Manuf. Process.* 73 (2022) 496–517, <https://doi.org/10.1016/j.jmapro.2021.11.036>.
- [58] Z. Zeng, M. Salehi, A. Kopp, S. Xu, M. Esmaily, N. Birbilis, Recent progress and perspectives in additive manufacturing of magnesium alloys, *J. Magnes. Alloys* 10 (6) (2022) 1511–1541, <https://doi.org/10.1016/j.jma.2022.03.001>.
- [59] D. Xie, F. Lv, Y. Yang, L. Shen, Z. Tian, C. Shuai, B. Chen, J. Zhao, A review on distortion and residual stress in additive manufacturing, *Chin. J. Mech. Eng. Addit. Manuf. Front.* 1 (3) (2022), <https://doi.org/10.1016/j.cjmeam.2022.100039>.
- [60] S.M. Orzolek, J.K. Semple, C.R. Fisher, Influence of processing on the microstructure of nickel aluminum bronze (NAB), *Addit. Manuf.* 56 (2022), <https://doi.org/10.1016/j.addma.2022.102859>.
- [61] R. Motallebi, Z. Savaedi, H. Mirzadeh, Post-processing heat treatment of lightweight magnesium alloys fabricated by additive manufacturing: a review, *J. Mater. Res. Technol.* 20 (2022) 1873–1892, <https://doi.org/10.1016/j.jmrt.2022.07.154>.
- [62] Y. Li, C. Su, J. Zhu, Comprehensive review of wire arc additive manufacturing: hardware system, physical process, monitoring, property characterization, application and future prospects, *Results. Eng.* 13 (2022), <https://doi.org/10.1016/j.rineng.2021.100330>.
- [63] M. Lalegani Dezaki, A. Serjouei, A. Zolfagharian, M. Fotouhi, M. Moradi, M.K. A. Ariffin, M. Bodaghi, A review on additive/subtractive hybrid manufacturing of directed energy deposition (DED) process, *Adv. Powder Mater.* 1 (4) (2022), <https://doi.org/10.1016/j.apmate.2022.100054>.
- [64] A. Kumar Sinha, S. Pramanik, K.P. Yagati, Research progress in arc based additive manufacturing of aluminium alloys – A review, *Measurement* 200 (2022), <https://doi.org/10.1016/j.measurement.2022.111672>.
- [65] L. Guo, L. Zhang, J. Andersson, O. Ojo, Additive manufacturing of 18 % nickel maraging steels: defect, structure and mechanical properties: A review, *J. Mater. Sci. Technol.* 120 (2022) 227–252, <https://doi.org/10.1016/j.jmst.2021.10.056>.
- [66] D. Ding, Z. Pan, S. Van Duin, H. Li, C.J.M. Shen, Fabricating superior NiAl bronze components through wire arc additive manufacturing, *Materials* 9 (8) (2016) 652, <https://doi.org/10.3390/ma9080652>.
- [67] F. Wang, S. Williams, M.J.T.i.j.o.a.m.t. Rush, Morphology investigation on direct current pulsed gas tungsten arc welded additive layer manufactured Ti6Al4V alloy, *Int. J. Adv. Manuf. Technol.* 57 (5) (2011) 597–603, <https://doi.org/10.1007/s00170-011-3299-1>.
- [68] Z. Pan, D. Ding, B. Wu, D. Cuiuri, H. Li, J. Norrish, Arc welding processes for additive manufacturing: A review, *Trans. Intell. Weld. Manuf.* (2018) 3–24, https://doi.org/10.1007/978-981-10-5355-9_1.
- [69] M.D. Barath Kumar, M. Manikandan, Assessment of process, parameters, residual stress mitigation, post treatments and finite element analysis simulations of wire arc additive manufacturing technique, *Met. Mater. Int.* 28 (1) (2021) 54–111, <https://doi.org/10.1007/s12540-021-01015-5>.
- [70] F. He, L. Yuan, H. Mu, M. Ros, D. Ding, Z. Pan, H. Li, Research and application of artificial intelligence techniques for wire arc additive manufacturing: a state-of-the-art review, *Robot. Comput. Integr. Manuf.* 82 (2023) 102525, <https://doi.org/10.1016/j.rcim.2023.102525>.
- [71] Z. Silvayeh, J. Domitner, M. Müller, P. Auer, C. Sommitsch, P. Mayr, Engineering approach for modeling the deformation and fracture behavior of thin welds, *Results. Eng.* 21 (2024) 101799, <https://doi.org/10.1016/j.rineng.2024.101799>.
- [72] V.T. Le, A preliminary study on gas metal arc welding-based additive manufacturing of metal parts, *Sci. Technol. Dev. J.* 23 (2019), <https://doi.org/10.32508/stdj.v23i1.1714>.
- [73] N. Kumar, H. Bhavsar, P. Mahesh, A.K. Srivastava, B.J. Bora, A. Saxena, A.R.J.M.C. Dixit, Physics, wire arc additive manufacturing—A revolutionary method in additive manufacturing, *Mater. Chem. Phys.* 285 (2022) 126144, <https://doi.org/10.1016/j.matchemphys.2022.126144>.
- [74] S. Pattanayak, S.K. Sahoo, Gas metal arc welding based additive manufacturing—A review, *CIRP. J. Manuf. Sci. Technol.* 33 (2021) 398–442, <https://doi.org/10.1016/j.cirpj.2021.04.010>.
- [75] X. Wang, Y. Shi, G. Yu, B. Liang, Y. Li, Groove-center detection in gas metal arc welding using a template-matching method, *Int. J. Adv. Manuf. Technol.* 86 (9–12) (2016) 2791–2801, <https://doi.org/10.1007/s00170-016-8389-7>.
- [76] N. Rodriguez, L. Vázquez, I. Huarte, E. Arruti, I. Taberero, P. Alvarez, Wire and arc additive manufacturing: a comparison between CMT and TopTIG processes applied to stainless steel, *Weld. World* 62 (5) (2018) 1083–1096, <https://doi.org/10.1007/s40194-018-0606-6>.
- [77] D.T. Sarathchandra, M.J. Davidson, G. Visvanathan, Parameters effect on SS304 beads deposited by wire arc additive manufacturing, *Mater. Manufacturing Processes* 35 (7) (2020) 852–858, <https://doi.org/10.1080/10426914.2020.1743852>.
- [78] X. Yang, J. Liu, Z. Wang, X. Lin, F. Liu, W. Huang, E. Liang, Microstructure and mechanical properties of wire and arc additive manufactured AZ31 magnesium alloy using cold metal transfer process, *Mater. Sci. Eng. A* 774 (2020) 138942, <https://doi.org/10.1016/j.msea.2020.138942>.
- [79] C. Xia, Z. Pan, J. Polden, H. Li, Y. Xu, S. Chen, Y. Zhang, A review on wire arc additive manufacturing: monitoring, control and a framework of automated system, *J. Manuf. Syst.* 57 (2020) 31–45, <https://doi.org/10.1016/j.jmsy.2020.08.008>.
- [80] T.-C. Chan, S.V. Medarametla, R. behera, Analyzing positional accuracy and structural efficiency in additive manufacturing systems with moving elements, *Structurs. Eng.* 23 (2024) 102344, <https://doi.org/10.1016/j.rineng.2024.102344>.
- [81] V. Kumar, A. Mandal, A.K. Das, S. Kumar, Parametric study and characterization of wire arc additive manufactured steel structures, *Int. J. Adv. Manuf. Technol.* 115 (5–6) (2021) 1723–1733, <https://doi.org/10.1007/s00170-021-07261-6>.
- [82] X. Wang, A. Wang, K. Wang, Y. Li, Process stability for GTAW-based additive manufacturing, *Rapid. Prototyp. J.* 25 (5) (2019) 809–819, <https://doi.org/10.1108/rpj-02-2018-0046>.
- [83] L.P. Raut, R.V. Taiwade, Wire Arc Additive Manufacturing: A comprehensive review and research directions, *J. Mater. Eng. Perform.* 30 (7) (2021) 4768–4791, <https://doi.org/10.1007/s11665-021-05871-5>.
- [84] D. Jafari, T.H.J. Vaneker, I. Gibson, Wire and arc additive manufacturing: opportunities and challenges to control the quality and accuracy of manufactured parts, *Mater. Des.* 202 (2021), <https://doi.org/10.1016/j.matdes.2021.109471>.
- [85] M. Bruggi, V. Laghi, T. Trombetti, Simultaneous design of the topology and the build orientation of wire-and-arc additively manufactured structural elements, *Comput. Struct.* 242 (2021) 106370, <https://doi.org/10.1016/j.compstruc.2020.106370>.
- [86] H. Pant, A. Arora, G.S. Gopakumar, U. Chadha, A. Saeidi, A.E. Patterson, Applications of wire arc additive manufacturing (WAAM) for aerospace component manufacturing, *Int. J. Adv. Manuf. Technol.* 127 (11–12) (2023) 4995–5011, <https://doi.org/10.1007/s00170-023-11623-7>.
- [87] M. Xu, S. Chen, T. Yuan, X. Jiang, H.J.J.o.A. Zhang, Composites, effect of thermal cycles on the microstructure and properties of the Al–Zn–Mg–Cu alloy during wire-arc additive manufacturing, *J. Alloys. Compd.* 928 (2022) 167172, <https://doi.org/10.1016/j.jallcom.2022.167172>.
- [88] K.L. Terrassa, T.R. Smith, S. Jiang, J.D. Sugar, J.M. Schoenung, Improving build quality in directed energy deposition by cross-hatching, *Mater. Sci. Eng. A* 765 (2019) 138269, <https://doi.org/10.1016/j.msea.2019.138269>.
- [89] T. DebRoy, H.L. Wei, J.S. Zuback, T. Mukherjee, J.W. Elmer, J.O. Milewski, A. M. Beese, A. Wilson-Heid, A. De, W. Zhang, Additive manufacturing of metallic components – Process, structure and properties, *Prog. Mater. Sci.* 92 (2018) 112–224, <https://doi.org/10.1016/j.pmatsci.2017.10.001>.
- [90] H.M. Khan, G. Özer, M.S. Yilmaz, E.J.A.J.f.s. Koc, Engineering, corrosion of additively manufactured metallic components: a review, *Arab. J. Sci. Eng.* 47 (5) (2022) 1–26, <https://doi.org/10.1007/s13369-021-06481-y>.
- [91] B. Wu, D. Ding, Z. Pan, D. Cuiuri, H. Li, J. Han, Z. Fei, Effects of heat accumulation on the arc characteristics and metal transfer behavior in Wire Arc Additive manufacturing of Ti6Al4V, *J. Mater. Process. Technol.* 250 (2017) 304–312, <https://doi.org/10.1016/j.jmatprotec.2017.07.037>.
- [92] D. Svetlizky, M. Das, B. Zheng, A.L. Vyatskikh, S. Bose, A. Bandyopadhyay, J. M. Schoenung, E.J. Lavernia, N. Eliaz, Directed energy deposition (DED) additive manufacturing: physical characteristics, defects, challenges and applications, *Mater. Today* (2021), <https://doi.org/10.1016/j.matod.2021.03.020>.
- [93] A. Shah, R. Aliyev, H. Zeidler, S. Krinke, A review of the recent developments and challenges in Wire arc additive manufacturing (WAAM) process, *J. Manuf. Mater. Process.* 7 (3) (2023), <https://doi.org/10.3390/jmmp7030097>.
- [94] T.A. Rodrigues, V. Duarte, R.M. Miranda, T.G. Santos, J.P. Oliveira, Current status and perspectives on wire and Arc Additive manufacturing (WAAM), *Materials* 12 (7) (2019), <https://doi.org/10.3390/ma12071121>.
- [95] Y. Koli, N. Yuvaraj, A. Sivanandam, Vipin, control of humping phenomenon and analyzing mechanical properties of Al–Si wire-arc additive manufacturing fabricated samples using cold metal transfer process, *Proc. Institut. Mech. Eng. Part C J. Mech. Eng. Sci.* 236 (2) (2021) 984–996, <https://doi.org/10.1177/0954406221998402>.
- [96] D. Yang, C. He, G. Zhang, Forming characteristics of thin-wall steel parts by double electrode GMAW based additive manufacturing, *J. Mater. Process. Technol.* 227 (2016) 153–160, <https://doi.org/10.1016/j.jmatprotec.2015.08.021>.
- [97] J. Xiong, G. Zhang, W. Zhang, Forming appearance analysis in multi-layer single-pass GMAW-based additive manufacturing, *Int. J. Adv. Manuf. Technol.* 80 (9–12) (2015) 1767–1776, <https://doi.org/10.1007/s00170-015-7112-4>.
- [98] L. Liu, Z. Zhuang, F. Liu, M. Zhu, Additive manufacturing of steel–bronze bimetal by shaped metal deposition: interface characteristics and tensile properties, *Int. J. Adv. Manuf. Technol.* 69 (9–12) (2013) 2131–2137, <https://doi.org/10.1007/s00170-013-5191-7>.
- [99] T. Abe, H. Sasahara, Dissimilar metal deposition with a stainless steel and nickel-based alloy using wire and arc-based additive manufacturing, *Precision Engineering*, 45 (2016), 387–395, [doi:10.1016/j.precisioneng.2016.03.016](https://doi.org/10.1016/j.precisioneng.2016.03.016).

- [100] H. Luo, X. Sun, L. Xu, W. He, X.J.T. Liang, A.M. Letters, A review on stress determination and control in metal-based additive manufacturing, *Theor. Appl. Mech. Lett.* 13 (1) (2022) 100396, <https://doi.org/10.1016/j.taml.2022.100396>.
- [101] B. Kumar, M.J.M. Manikandan, M. International, Assessment of process, parameters, residual stress mitigation, post treatments and finite element analysis simulations of wire arc additive manufacturing technique, 28 (1) (2022), 54–111.
- [102] M.L. Griffith, M.E. Schlienger, L.D. Harwell, M.S. Oliver, M.D. Baldwin, M. T. Ensz, M. Essien, J. Brooks, C.V. Robino, J.E. Smugeresky, W.H. Hofmeister, M. J. Wert, D.V. Nelson, Understanding thermal behavior in the LENS process, *Mater. Des.* 20 (2-3) (1999) 107–113, [https://doi.org/10.1016/s0261-3069\(99\)00016-3](https://doi.org/10.1016/s0261-3069(99)00016-3).
- [103] F. Lia, J.Z. Park, J.S. Keist, S. Joshi, R.P. Martukanitz, Thermal and microstructural analysis of laser-based directed energy deposition for Ti-6Al-4V and inconel 625 deposits, *Mater. Sci. Eng. A* 717 (2018) 1–10, <https://doi.org/10.1016/j.msea.2018.01.060>.
- [104] D.A. Kriczky, J. Irwin, E.W. Reutzler, P. Michaleris, A.R. Nassar, J. Craig, 3D spatial reconstruction of thermal characteristics in directed energy deposition through optical thermal imaging, *J. Mater. Process. Technol.* 221 (2015) 172–186, <https://doi.org/10.1016/j.jmatprotec.2015.02.021>.
- [105] J. Ding, P. Colegrove, J. Mehen, S. Ganguly, P.M. Sequeira Almeida, F. Wang, S. Williams, Thermo-mechanical analysis of Wire and Arc Additive layer manufacturing process on large multi-layer parts, *Comput. Mater. Sci.* 50 (12) (2011) 3315–3322, <https://doi.org/10.1016/j.commatsci.2011.06.023>.
- [106] W. Wu, A.D. Stoica, K.D. Berry, M.J. Frost, H.D. Skorpenske, K.J.A.P.L. An, PIND: high spatial resolution by pinhole neutron diffraction, *Appl. Phys. Lett.* 112 (25) (2018) 253501, <https://doi.org/10.1063/1.5026066>.
- [107] T. LeBrun, T. Nakamoto, K. Horikawa, H. Kobayashi, Effect of retained austenite on subsequent thermal processing and resultant mechanical properties of selective laser melted 17–4 PH stainless steel, *Mater. Des.* 81 (2015) 44–53, <https://doi.org/10.1016/j.matdes.2015.05.026>.
- [108] M. Alimardani, E. Toyserkani, J.P. Huissoun, C.P. Paul, On the delamination and crack formation in a thin wall fabricated using laser solid freeform fabrication process: an experimental–numerical investigation, *Opt. Lasers. Eng.* 47 (11) (2009) 1160–1168, <https://doi.org/10.1016/j.optlaseng.2009.06.010>.
- [109] S.-H. Li, P. Kumar, S. Chandra, U.J.I.M.R. Ramamurthy, Directed energy deposition of metals: processing, microstructures, and mechanical properties, *Int. Mater. Rev.* 68 (6) (2022) 1–43, <https://doi.org/10.1080/09506608.2022.2097411>.
- [110] N.S. Rossini, M. Dassisti, K.Y. Benyounis, A.G. Olabi, Methods of measuring residual stresses in components, *Mater. Des.* 35 (2012) 572–588, <https://doi.org/10.1016/j.matdes.2011.08.022>.
- [111] P.J. Withers, H.K.D.H. Bhadeshia, Residual stress. Part 1 – Measurement techniques, *Mater. Sci. Technol.* 17 (4) (2001) 355–365, <https://doi.org/10.1179/026708301101509980>.
- [112] R. Pokharel, A. Patra, D.W. Brown, B. Clausen, S.C. Vogel, G.T. Gray, An analysis of phase stresses in additively manufactured 304L stainless steel using neutron diffraction measurements and crystal plasticity finite element simulations, *Int. J. Plast.* 121 (2019) 201–217, <https://doi.org/10.1016/j.ijplas.2019.06.005>.
- [113] A. Avanzini, Fatigue behavior of additively manufactured stainless steel 316L, *Materials* 16 (1) (2022) 65, <https://doi.org/10.3390/ma16010065>.
- [114] M.A. Mahmood, D. Chioibas, A. Ur Rehman, S. Mihai, A.C.J.M. Popescu, Post-processing techniques to enhance the quality of metallic parts produced by additive manufacturing, *Metals* 12 (1) (2022) 77, <https://doi.org/10.3390/met12010077>.
- [115] N. Eliaz, Corrosion of metallic biomaterials: A review, *Materials* 12 (3) (2019) 407, <https://doi.org/10.3390/ma12030407>.
- [116] P. Kobryn, S. Semiatin, Mechanical properties of laser-deposited Ti-6Al-4V, in: 2001 International Solid Freeform Fabrication Symposium, 2001.
- [117] G. Kasperovich, J. Haubrich, J. Gussone, G. Requena, Correlation between porosity and processing parameters in TiAl6V4 produced by selective laser melting, *Mater. Des.* 105 (2016) 160–170, <https://doi.org/10.1016/j.matdes.2016.05.070>.
- [118] D. Herzog, V. Seyda, E. Wycisk, C.J.A.M. Emmelmann, Additive manufacturing of metals, *Acta Mater.* 117 (2016) 371–392, <https://doi.org/10.1016/j.actamat.2016.07.019>.
- [119] A. Busachi, J. Erkoyuncu, P. Colegrove, F. Martina, J. Ding, Designing a WAAM based manufacturing system for defence applications, *Procedia CIRP*. 37 (2015) 48–53, <https://doi.org/10.1016/j.procir.2015.08.085>.
- [120] J. Lizarazu, E. Harirchian, U.A. Shaik, M. Shareef, A. Antoni-Zdziobek, T. Lahmer, Application of machine learning-based algorithms to predict the stress-strain curves of additively manufactured mild steel out of its microstructural characteristics, *Results. Eng.* 20 (2023) 101587, <https://doi.org/10.1016/j.rineng.2023.101587>.
- [121] Effect of process parameters on the formation of lack of fusion in directed energy deposition of Ti-6Al-4V alloy, *J. Weld. Join.* 37 (6) (2019) 579–584, <https://doi.org/10.3345/kjp.2019.37.6.579>.
- [122] C. Qiu, N.J.E. Adkins, M.M. Attallah, Microstructure and tensile properties of selectively laser-melted and of HIPed laser-melted Ti-6Al-4V, *Mater. Sci. Eng. A* 578 (2013) 230–239, <https://doi.org/10.1016/j.msea.2013.04.099>.
- [123] C. Zhao, N.D. Parab, X. Li, K. Fezzaa, W. Tan, A.D. Rollett, T.J.S. Sun, Critical instability at moving keyhole tip generates porosity in laser melting, *Science* (1979) 370 (6520) (2020) 1080–1086, <https://doi.org/10.1126/science.abd1587>.
- [124] A. Dass, A. Moridi, State of the art in directed energy deposition: from additive manufacturing to materials design, *Coatings* 9 (7) (2019) 418, <https://doi.org/10.3390/coatings9070418>.
- [125] J.A. Slotwinski, E.J. Garboczi, K.M. Hebenstreit, Porosity measurements and analysis for metal additive manufacturing process control, *J. Res. Natl. Inst. Stand. Technol.* 119 (2014) 494–528, <https://doi.org/10.6028/jres.119.019>.
- [126] W. Tillmann, C. Schaak, J. Nellesen, M. Schaper, M.E. Aydinöz, K.P. Hoyer, Hot isostatic pressing of IN718 components manufactured by selective laser melting, *Addit. Manuf.* 13 (2017) 93–102, <https://doi.org/10.1016/j.addma.2016.11.006>.
- [127] S.R. Singh, P. Khanna, Wire arc additive manufacturing (WAAM): A new process to shape engineering materials, *Mater. Today Proc.* 44 (2021) 118–128, <https://doi.org/10.1016/j.matpr.2020.08.030>.
- [128] M.B. Hesari, R. Beygi, L.F.M. da Silva, Role of SiC powder in reducing the porosity and increasing the carbon content in wire arc additive manufacturing of carbon steel, in: A.J.M. Ferreira, L.F.M. da Silva (Eds.), 1st International Conference on Mechanics of Solids 2022, Springer International Publishing, Cham, 2023, pp. 17–29.
- [129] D. Peng, V.K. Champagne, A.S.M. Ang, A. Birt, A. Michelson, S. Pinches, R. Jones, Computing the durability of WAAM 18Ni-250 maraging steel specimens with surface breaking porosity, *Crystals*. (Basel) 13 (3) (2023), <https://doi.org/10.3390/cryst13030443>.
- [130] R. Zhang, W. Li, Y. Jiao, C. Paniagua, Y. Ren, H. Lu, Porosity evolution under increasing tension in wire-arc additively manufactured aluminum using in-situ micro-computed tomography and convolutional neural network, *Scr. Mater.* 225 (2023) 115172, <https://doi.org/10.1016/j.scriptamat.2022.115172>.
- [131] Y. Wei, F. Liu, F. Liu, D. Yu, Q. You, C. Huang, Z. Wang, W. Jiang, X. Lin, X. Hu, Effect of arc oscillation on porosity and mechanical properties of 2319 aluminum alloy fabricated by CMT-wire arc additive manufacturing, *J. Mater. Res. Technol.* 24 (2023) 3477–3490, <https://doi.org/10.1016/j.jmrt.2023.03.203>.
- [132] K.J. Sandeep, P.J. Teja, A.K. Choudhary, R. Jain, Development of correlation between temperature, liquid life span, molten pool, and porosity during Wire Arc Additive Manufacturing: a finite element approach, *CIRP. J. Manuf. Sci. Technol.* 38 (2022) 274–287, <https://doi.org/10.1016/j.cirpj.2022.05.002>.
- [133] Y. Guo, Q. Han, J. Hu, X. Yang, P. Mao, J. Wang, S. Sun, Z. He, J. Lu, C. Liu, Comparative study on wire-arc additive manufacturing and conventional casting of Al-Si alloys: porosity, microstructure and mechanical property, *Acta Metallurgica Sinica* 35 (3) (2021) 475–485, <https://doi.org/10.1007/s40195-021-01314-1>.
- [134] Y. Yan, J. Si, X. Di, Y. Guo, Q. Han, C. Liu, Minimizing porosity and optimizing microstructure of hot-wire arc additive manufactured Al-Cu-Mg-Ag alloy for strength increment, *J. Manuf. Process.* 118 (2024) 89–102, <https://doi.org/10.1016/j.jmapro.2024.03.053>.
- [135] M. Shami, A.K. Syed, V. Janik, R. Biswal, X. Zhang, The role of microstructure and local crystallographic orientation near porosity defects on the high cycle fatigue life of an additive manufactured Ti-6Al-4V, *Mater. Charact.* 169 (2020) 110576, <https://doi.org/10.1016/j.matchar.2020.110576>.
- [136] K. Touileb, A. Ouis, A.C. Hedhibi, A. Ibrahim, H.S.J.M. Abdo, Effects of metal and fluoride powders deposition on hot-cracking susceptibility of 316L stainless steel in TIG welding, *Metals*. (Basel) 12 (7) (2022) 1225, <https://doi.org/10.3390/met12071225>.
- [137] S. Sridar, N. Sargent, X. Wang, M.A. Klecka, W.J.M. Xiong, Determination of location-specific solidification cracking susceptibility for a mixed dissimilar alloy processed by wire-arc additive manufacturing, *Metals*. 12 (2) (2022) 284, <https://doi.org/10.3390/met12020284>.
- [138] M. Xu, H. Zhang, T. Yuan, Z. Yan, S.J.M.C. Chen, Microstructural characteristics and cracking mechanism of AlCu alloys in wire arc additive manufacturing, *Mater. Charact.* 197 (2023) 112677, <https://doi.org/10.1016/j.matchar.2023.112677>.
- [139] W.J. Sames, F.A. List, S. Pannala, R.R. Dehoff, S.S. Babu, The metallurgy and processing science of metal additive manufacturing, *Int. Mater. Rev.* 61 (5) (2016) 315–360, <https://doi.org/10.1080/09506608.2015.1116649>.
- [140] K. Mizukami, R. Imanishi, H. Matsushita, Y. Koga, Design and additive manufacturing of elastic metamaterials with 3D lever-type inertial amplification mechanisms for mitigation of low-frequency vibration, *Results. Eng.* 20 (2023) 101389, <https://doi.org/10.1016/j.rineng.2023.101389>.
- [141] H.L. Wei, T. Mukherjee, W. Zhang, J.S. Zuback, G.L. Knapp, A. De, T. DebRoy, Mechanistic models for additive manufacturing of metallic components, *Prog. Mater. Sci.* 116 (2021) 100703, <https://doi.org/10.1016/j.pmatsci.2020.100703>.
- [142] S.J.J. Kou, Solidification and liquation cracking issues in welding, *Jom* 55 (6) (2003) 37–42, <https://doi.org/10.1007/s11837-003-0137-4>.
- [143] B.D. Bankong, T.E. Abioye, T.O. Olugbade, H. Zuhailawati, O.O. Gbadeyan, T. I. Ogedengbe, Review of post-processing methods for high-quality wire arc additive manufacturing, *Mater. Sci. Technol.* 39 (2) (2023) 129–146, <https://doi.org/10.1080/02670836.2022.2110223>.
- [144] J. Zhang, X. Wang, S. Paddea, X. Zhang, Fatigue crack propagation behaviour in wire+arc additive manufactured Ti-6Al-4V: effects of microstructure and residual stress, *Mater. Des.* 90 (2016) 551–561, <https://doi.org/10.1016/j.matdes.2015.10.141>.
- [145] C.E. Seow, J. Zhang, H.E. Coules, G. Wu, C. Jones, J. Ding, S. Williams, Effect of crack-like defects on the fracture behaviour of Wire + arc additively manufactured nickel-base Alloy 718, *Addit. Manuf.* 36 (2020) 101578, <https://doi.org/10.1016/j.addma.2020.101578>.
- [146] N. Kozamernik, D. Bračun, D. Klobčar, WAAM system with interpass temperature control and forced cooling for near-net-shape printing of small metal components, *Int. J. Adv. Manuf. Technol.* 110 (7-8) (2020) 1955–1968, <https://doi.org/10.1007/s00170-020-05958-8>.
- [147] L. Vázquez, N. Rodríguez, I. Rodríguez, E. Alberdi, P. Álvarez, Influence of interpass cooling conditions on microstructure and tensile properties of Ti-6Al-4V

- parts manufactured by WAAM, *Welding in the World* 64 (8) (2020) 1377–1388, <https://doi.org/10.1007/s40194-020-00921-3>.
- [148] J. Lettori, R. Raffaelli, P. Bilancia, M. Peruzzini, M.J.T.L.J.o.A.M.T. Pellicciari, A review of geometry representation and processing methods for cartesian and multi-axial robot-based additive manufacturing, *Int. J. Adv. Manuf. Technol.* 123 (11) (2022) 1–28, <https://doi.org/10.1007/s00170-022-10432-8>.
- [149] D. Ding, Z. Pan, D. Cuiuri, H. Li, Process planning for robotic wire and arc additive manufacturing, in: *2015 IEEE 10th Conference on Industrial Electronics and Applications (ICIEA)*, IEEE, 2015, pp. 2000–2003.
- [150] A.A. Akinwande, O.A. Balogun, A.A. Adediran, O.S. Adesina, V. Romanovski, T. C. Jen, Experimental analysis, statistical modeling, and parametric optimization of quinary-(CoCrFeMnNi)100-x/TiCx high-entropy-alloy (HEA) manufactured by laser additive manufacturing, *Results. Eng.* 17 (2023) 100802, <https://doi.org/10.1016/j.rineng.2022.100802>.
- [151] D. Ding, Z. Pan, D. Cuiuri, H. Li, A multi-bead overlapping model for robotic wire and arc additive manufacturing (WAAM), *Robot. Comput. Integr. Manuf.* 31 (2015) 101–110, <https://doi.org/10.1016/j.rcim.2014.08.008>.
- [152] M. Srivastava, S. Rathee, Additive manufacturing: recent trends, applications and future outlooks, *Progr. Additive Manuf.* 7 (2) (2022) 261–287, <https://doi.org/10.1007/s40964-021-00229-8>.
- [153] U. Tripathi, N. Saini, R.S. Mulik, M.M. Mahapatra, Effect of build direction on the microstructure evolution and their mechanical properties using GTAW based wire arc additive manufacturing, *CIRP. J. Manuf. Sci. Technol.* 37 (2022) 103–109, <https://doi.org/10.1016/j.cirpj.2022.01.010>.
- [154] S. Singh, S.K. Sharma, D.W. Rathod, A review on process planning strategies and challenges of WAAM, *Mater. Today Proc.* 47 (2021) 6564–6575, <https://doi.org/10.1016/j.matpr.2021.02.632>.
- [155] B. Ahmad, X. Zhang, H. Guo, M.E. Fitzpatrick, L.M. Neto, S. Williams, Influence of deposition strategies on residual stress in wire + arc additive manufactured titanium Ti-6Al-4V, *Metals* 12 (2) (2022), <https://doi.org/10.3390/met12020253>.
- [156] M. Arana, E. Ukar, I. Rodriguez, D. Aguilar, P. Álvarez, Influence of deposition strategy and heat treatment on mechanical properties and microstructure of 2319 aluminium WAAM components, *Mater. Des.* 221 (2022) 110974, <https://doi.org/10.1016/j.matdes.2022.110974>.
- [157] M. Chaturvedi, E. Scutelnicu, C.C. Rusu, L.R. Mistodie, D. Mihailescu, A. V. Subbiah, Wire Arc Additive manufacturing: review on recent findings and challenges in industrial applications and materials characterization, *Metals* 11 (6) (2021), <https://doi.org/10.3390/met11060939>.
- [158] R. Chaudhari, H. Parmar, J. Vora, V.K.J.M. Patel, Parametric study and investigations of bead geometries of GMAW-based wire-arc additive manufacturing of 316L stainless steels, *Metals* (Basel) 12 (7) (2022) 1232, <https://doi.org/10.3390/met12071232>.
- [159] S. Suryakumar, K.P. Karunakaran, A. Bernard, U. Chandrasekhar, N. Raghavender, D. Sharma, Weld bead modeling and process optimization in Hybrid Layered Manufacturing, *Comput. Aided Des.* 43 (4) (2011) 331–344, <https://doi.org/10.1016/j.cad.2011.01.006>.
- [160] J. Xiong, G. Zhang, H. Gao, L. Wu, Modeling of bead section profile and overlapping beads with experimental validation for robotic GMAW-based rapid manufacturing, *Robot. Comput. Integr. Manuf.* 29 (2) (2013) 417–423, <https://doi.org/10.1016/j.rcim.2012.09.011>.
- [161] Y. Li, Y. Sun, Q. Han, G. Zhang, I. Horváth, Enhanced beads overlapping model for wire and arc additive manufacturing of multi-layer multi-bead metallic parts, *J. Mater. Process. Technol.* 252 (2018) 838–848, <https://doi.org/10.1016/j.jmatprotec.2017.10.017>.
- [162] S.H. Lee, Optimization of cold metal transfer-based wire arc additive manufacturing processes using gaussian process regression, *Metals* (Basel) 10 (4) (2020), <https://doi.org/10.3390/met10040461>.
- [163] K. Omata, Screening of new additives of active-carbon-supported heteropoly acid catalyst for Friedel-Crafts reaction by gaussian process regression, *Ind. Eng. Chem. Res.* 50 (19) (2011) 10948–10954, <https://doi.org/10.1021/ie102477y>.
- [164] U. Reissen, R. Sharma, S. Mann, L. Oster, Increasing the manufacturing efficiency of WAAM by advanced cooling strategies, *Weld. World* 64 (8) (2020) 1409–1416, <https://doi.org/10.1007/s40194-020-00930-2>.
- [165] J. Müller, M. Grabowski, C. Müller, J. Hensel, J. Unglaub, K. Thiele, H. Kloft, K. Dilger, Design and parameter identification of wire and arc additively manufactured (WAAM) steel bars for use in construction, *Metals* 9 (7) (2019), <https://doi.org/10.3390/met9070725>.
- [166] A. Dash, L. Squires, J.D. Avila, S. Bose, A. Bandyopadhyay, Influence of active cooling on microstructure and mechanical properties of wire arc additively manufactured mild steel, *Front. Mech. Eng.* 9 (2023), <https://doi.org/10.3389/fmech.2023.1130407>.
- [167] B. Panda, K. Shankhwar, A. Garg, M.M. Savalani, Evaluation of genetic programming-based models for simulating bead dimensions in wire and arc additive manufacturing, *J. Intell. Manuf.* 30 (2) (2019) 809–820, <https://doi.org/10.1007/s10845-016-1282-2>.
- [168] K.P. Prajadhiana, Y.H.P. Manurung, M.S. Adenan, M.F. Mat, Investigation of material model effect on WAAM SS316L using numerical simulation, in: M. N. Osman Zahid, A.S. Abdul Sani, M.R. Mohamad Yasin, Z. Ismail, N.A. Che Lah, F. Mohd Turan (Eds.), *Recent Trends in Manufacturing and Materials Towards Industry 4.0*, Springer Singapore, Singapore, 2021, pp. 329–341.
- [169] B.P. Nagasai, S. Malarvizhi, V. Balasubramanian, Effect of welding processes on mechanical and metallurgical characteristics of carbon steel cylindrical components made by wire arc additive manufacturing (WAAM) technique, *CIRP. J. Manuf. Sci. Technol.* 36 (2022) 100–116, <https://doi.org/10.1016/j.cirpj.2021.11.005>.
- [170] J. Kim, J. Kim, J. Cheon, C. Ji, Effect of filler metal type on microstructure and mechanical properties of fabricated NiAl bronze alloy using wire arc additive manufacturing system, *Metals* (Basel) 11 (3) (2021), <https://doi.org/10.3390/met11030513>.
- [171] F. Marefat, A. Kapil, S.A. Banaee, P. Van Rymentant, A. Sharma, Evaluating shielding gas-filler wire interaction in bi-metallic wire arc additive manufacturing (WAAM) of creep resistant steel-stainless steel for improved process stability and build quality, *J. Manuf. Process.* 88 (2023) 110–124, <https://doi.org/10.1016/j.jmapro.2023.01.046>.
- [172] L.J. da Silva, F.M. Scotti, D.B. Fernandes, R.P. Reis, A. Scotti, Effect of O2 content in argon-based shielding gas on arc wandering in WAAM of aluminum thin walls, *CIRP. J. Manuf. Sci. Technol.* 32 (2021) 338–345, <https://doi.org/10.1016/j.cirpj.2021.01.018>.
- [173] H. Lockett, J. Ding, S. Williams, F. Martina, Design for Wire + arc Additive manufacture: design rules and build orientation selection, *J. Eng. Des.* 28 (7-9) (2017) 568–598, <https://doi.org/10.1080/09544828.2017.1365826>.
- [174] B. Liu, H. Shen, Z. Zhou, J. Jin, J. Fu, Research on support-free WAAM based on surface/interior separation and surface segmentation, *J. Mater. Process. Technol.* 297 (2021) 117240, <https://doi.org/10.1016/j.jmatprotec.2021.117240>.
- [175] L. Yuan, Z. Pan, D. Ding, Z. Yu, S. van Duijn, H. Li, W. Li, J. Norrish, Fabrication of metallic parts with overhanging structures using the robotic wire arc additive manufacturing, *J. Manuf. Process.* 63 (2021) 24–34, <https://doi.org/10.1016/j.jmapro.2020.03.018>.
- [176] M. Cheepu, V.C.J.T.o.t.I.I.o.M. Kantumuchu, Numerical simulations of the effect of heat input on microstructural growth for MIG-based wire arc additive manufacturing of Inconel 718, *Trans. Ind. Institute Metals* 76 (2) (2022) 1–9, <https://doi.org/10.1007/s12666-022-02749-5>.
- [177] C. Zhang, Z. Qiu, H. Zhu, Z. Wang, O. Muránsky, M. Ionescu, Z. Pan, J. Xi, H.J. M. Li, On the effect of heat input and interpass temperature on the performance of inconel 625 alloy deposited using wire arc additive manufacturing-cold metal transfer process, *Metals* 12 (1) (2022) 46, <https://doi.org/10.3390/met12010046>.
- [178] N.A. Rosli, M.R. Alkahari, M.F.b. Abdollah, S. Maidin, F.R. Ramli, S.G. Herawan, Review on effect of heat input for wire arc additive manufacturing process, *J. Mater. Res. Technol.* 11 (2021) 2127–2145, <https://doi.org/10.1016/j.jmrt.2021.02.002>.
- [179] A.S. Yildiz, K. Davut, B. Koc, O. Yilmaz, Wire arc additive manufacturing of high-strength low alloy steels: study of process parameters and their influence on the bead geometry and mechanical characteristics, *Int. J. Adv. Manuf. Technol.* 108 (11-12) (2020) 3391–3404, <https://doi.org/10.1007/s00170-020-05482-9>.
- [180] F. Youheng, W. Guilan, Z. Haiou, L. Liye, Optimization of surface appearance for wire and arc additive manufacturing of Bainite steel, *Int. J. Adv. Manuf. Technol.* 91 (1-4) (2016) 301–313, <https://doi.org/10.1007/s00170-016-9621-1>.
- [181] V.A. Hosseini, M. Höglström, K. Hurlig, M.A. Valiente Bermejo, L.-E. Stridh, L. Karlsson, Wire-arc additive manufacturing of a duplex stainless steel: thermal cycle analysis and microstructure characterization, *Weld. World* 63 (4) (2019) 975–987, <https://doi.org/10.1007/s40194-019-00735-y>.
- [182] C. Su, X. Chen, C. Gao, Y. Wang, Effect of heat input on microstructure and mechanical properties of Al-Mg alloys fabricated by WAAM, *Appl. Surf. Sci.* 486 (2019) 431–440, <https://doi.org/10.1016/j.apsusc.2019.04.255>.
- [183] Z. Li, C. Liu, T. Xu, L. Ji, D. Wang, J. Lu, S. Ma, H. Fan, Reducing arc heat input and obtaining equiaxed grains by hot-wire method during arc additive manufacturing titanium alloy, *Mater. Sci. Eng. A* 742 (2019) 287–294, <https://doi.org/10.1016/j.msea.2018.11.022>.
- [184] V. Gorniyakov, J. Ding, Y. Sun, S.J.M. Williams, Design, understanding and designing post-build rolling for mitigation of residual stress and distortion in wire arc additively manufactured components, *Mater. Des.* 213 (2022) 110335, <https://doi.org/10.1016/j.matdes.2021.110335>.
- [185] P.A. Colegrove, H.E. Coules, J. Fairman, F. Martina, T. Kashoob, H. Mamash, L. D. Cozzolino, Microstructure and residual stress improvement in wire and arc additively manufactured parts through high-pressure rolling, *J. Mater. Process. Technol.* 213 (10) (2013) 1782–1791, <https://doi.org/10.1016/j.jmatprotec.2013.04.012>.
- [186] Y. Fu, H. Zhang, G. Wang, H. Wang, Investigation of mechanical properties for hybrid deposition and micro-rolling of bainite steel, *J. Mater. Process. Technol.* 250 (2017) 220–227, <https://doi.org/10.1016/j.jmatprotec.2017.07.023>.
- [187] P. Dirisu, G. Supriyo, F. Martina, X. Xu, S. Williams, Wire plus arc additive manufactured functional steel surfaces enhanced by rolling, *Int. J. Fatigue* 130 (2020), <https://doi.org/10.1016/j.ijfatigue.2019.105237>.
- [188] T.A. Rodrigues, V. Duarte, R.M. Miranda, T.G. Santos, J.P. Oliveira, Current status and perspectives on wire and Arc Additive manufacturing (WAAM), *Materials* 12 (7) (2019), <https://doi.org/10.3390/ma12071121>.
- [189] M. Rafieezad, M. Ghaffari, A. Vahedi Nemani, A. Nasiri, Microstructural evolution and mechanical properties of a low-carbon low-alloy steel produced by wire arc additive manufacturing, *Int. J. Adv. Manuf. Technol.* 105 (5-6) (2019) 2121–2134, <https://doi.org/10.1007/s00170-019-04393-8>.
- [190] K. Hajizadeh, K.J. Kurzydowski, Microstructure evolution and mechanical properties of AISI 316H austenitic stainless steel processed by warm Multi-pass ECAP, *Phys. Metals Metallogr.* 122 (9) (2021) 931–938, <https://doi.org/10.1134/s0031918x21300013>.
- [191] D. rahmatgadi, g. faragi, r. hashemi, Review on accumulative roll bonding of ultrafine grained and nanostructured sheets, *%J Iran. J. Manuf. Eng.* 6 (4) (2019) 37–51.
- [192] X. Bai, H. Zhang, G. Wang, Modeling of the moving induction heating used as secondary heat source in weld-based additive manufacturing, *Int. J. Adv. Manuf. Technol.* 77 (1-4) (2014) 717–727, <https://doi.org/10.1007/s00170-014-6475-2>.

- [193] J. Xiong, Y. Lei, R. Li, Finite element analysis and experimental validation of thermal behavior for thin-walled parts in GMAW-based additive manufacturing with various substrate preheating temperatures, *Appl. Therm. Eng.* 126 (2017) 43–52, <https://doi.org/10.1016/j.applthermaleng.2017.07.168>.
- [194] Q. Wu, T. Mukherjee, A. De, T. DebRoy, Residual stresses in wire-arc additive manufacturing – Hierarchy of influential variables, *Addit. Manuf.* 35 (2020), <https://doi.org/10.1016/j.addma.2020.101355>.
- [195] B. Wu, Z. Pan, D. Ding, D. Cuiuri, H. Li, Z. Fei, The effects of forced interpass cooling on the material properties of wire arc additively manufactured Ti6Al4V alloy, *J. Mater. Process. Technol.* 258 (2018) 97–105, <https://doi.org/10.1016/j.jmatprotec.2018.03.024>.
- [196] D. Weisz-Patrault, P. Margerit, A.J.A.M. Constantinescu, Residual stresses in thin walled-structures manufactured by directed energy deposition: In-situ measurements, fast thermo-mechanical simulation and buckling, *Addit. Manuf.* 56 (2022) 102903, <https://doi.org/10.1016/j.addma.2022.102903>.
- [197] H. Geng, J. Li, J. Xiong, X. Lin, Optimisation of interpass temperature and heat input for wire and arc additive manufacturing 5A06 aluminium alloy, *Sci. Technol. of Weld. Join.* 22 (6) (2016) 472–483, <https://doi.org/10.1080/13621718.2016.1259031>.
- [198] M. Anis, K. Derekar, J. Lawrence, G. Melton, A. Addison, X. Zhang, L. Xu, B. Munir, Influence of interpass temperature on wire arc additive manufacturing (WAAM) of aluminium alloy components, *MATEC Web of Confer.* 269 (2019), <https://doi.org/10.1051/mateconf/201926905001>.
- [199] S. Panicker, H.P. Nagarajan, J. Tuominen, M. Patnamsetty, E. Coatanéa, K.R.J.M. S. Haapala, E. A, Investigation of thermal influence on weld microstructure and mechanical properties in wire and arc additive manufacturing of steels, *Mater. Sci. Eng. A* 853 (2022) 143690, <https://doi.org/10.1016/j.msea.2022.143690>.
- [200] V.T. Le, V.T. Le, An investigation on the impact of the interpass-cooling time on the metallurgy of wire-arc-additive-manufacturing SS308L components, proceedings of the 2nd Annual International Conference on Material, Mach. Methods Sustain. Dev. (MMMS2020) (2021) 196–201, https://doi.org/10.1007/978-3-030-69610-8_26.
- [201] W. Hackenhaar, J.A.E. Mazzaferro, F. Montevecchi, G. Campatelli, An experimental-numerical study of active cooling in wire arc additive manufacturing, *J. Manuf. Process.* 52 (2020) 58–65, <https://doi.org/10.1016/j.jmapro.2020.01.051>.
- [202] G. Casalino, M. Moradi, M.K. Moghadam, A. Khorram, P. Perulli, Experimental and numerical study of AISI 4130 steel surface hardening by pulsed Nd:YAG laser, *Materials* 12 (19) (2019) 3136, <https://doi.org/10.3390/ma12193136>.
- [203] B. Bankong, T. Abioye, T. Olugbade, H. Zuhailawati, O. Gbadeyan, T.J.M.S. Ogedengbe, Technology, review of post-processing methods for high-quality wire arc additive manufacturing, (2022), 1–18.
- [204] M. Srivastava, S. Rathee, A. Tiwari, M.J.M.C. Dongre, Physics, wire arc additive manufacturing of metals: A review on processes, materials and their behaviour, (2022), 126988.
- [205] B. Tomar, S. Shiva, T.J.M.T.C. Nath, A review on wire arc additive manufacturing: processing parameters, defects, quality improvement and recent advances, (2022), 103739.
- [206] R. Motallebi, Z. Savaedi, H.J.J.o.M.R. Mirzadeh, Technology, post-processing heat treatment of lightweight magnesium alloys fabricated by additive manufacturing: A review, *J. Mater. Res. Technol.* 20 (2022) 1873–1892, <https://doi.org/10.1016/j.jmrt.2022.07.154>.
- [207] A. Vahedi Nemani, M. Ghaffari, S. Salahi, A. Nasiri, Effects of post-printing heat treatment on the microstructure and mechanical properties of a wire arc additive manufactured 420 martensitic stainless steel part, *Mater. Sci. Eng. A* 813 (2021), <https://doi.org/10.1016/j.msea.2021.141167>.
- [208] A. Vahedi Nemani, M. Ghaffari, A. Nasiri, On the post-printing heat treatment of a wire arc additively manufactured ER70S part, *Materials* 13 (12) (2020), <https://doi.org/10.3390/ma13122795>.
- [209] K. Li, M.A. Klecka, S. Chen, W. Xiong, Wire-arc additive manufacturing and post-heat treatment optimization on microstructure and mechanical properties of grade 91 steel, *Addit. Manuf.* 37 (2021), <https://doi.org/10.1016/j.addma.2020.101734>.
- [210] M.R.U. Ahsan, A.N.M. Tanvir, G.-J. Seo, B. Bates, W. Hawkins, C. Lee, P.K. Liaw, M. Noakes, A. Nycz, D.B. Kim, Heat-treatment effects on a bimetallic additively-manufactured structure (BAMS) of the low-carbon steel and austenitic-stainless steel, *Addit. Manuf.* 32 (2020), <https://doi.org/10.1016/j.addma.2020.101036>.
- [211] L. Tonelli, R. Sola, V. Laghi, M. Palermo, T. Trombetti, L. Ceschini, Influence of interlayer forced air cooling on microstructure and mechanical properties of wire arc additively manufactured 304L austenitic stainless steel, *Steel. Res. Int.* 92 (11) (2021), <https://doi.org/10.1002/srin.202100175>.
- [212] C. Ma, Y. Liu, C. Li, H. Dong, D. Li, X. Wu, P. Liu, Q. Sun, H. Jin, F. Zhang, Mechanical properties of carbon steel by compound arc and vibration shock forging-rolling, *J. Manuf. Process.* 60 (2020) 11–22, <https://doi.org/10.1016/j.jmapro.2020.10.005>.
- [213] X. Xu, S. Ganguly, J. Ding, P. Dirisu, F. Martina, X. Liu, S.W. Williams, Improving mechanical properties of wire plus arc additively manufactured maraging steel through plastic deformation enhanced aging response, *Mater. Sci. Eng. A* 747 (2019) 111–118, <https://doi.org/10.1016/j.msea.2018.12.114>.
- [214] J.R. Hönnige, P.A. Colegrove, S. Ganguly, E. Eimer, S. Kabra, S. Williams, Control of residual stress and distortion in aluminium wire + arc additive manufacture with rolling, additive manufacturing, 22 (2018), 775–783, [doi:10.1016/j.addma.2018.06.015](https://doi.org/10.1016/j.addma.2018.06.015).
- [215] M.Y. Liu, B. Shi, C. Wang, S.K. Ji, X. Cai, H.W. Song, Normal Hall–Petch behavior of mild steel with submicron grains, *Mater. Lett.* 57 (19) (2003) 2798–2802, [https://doi.org/10.1016/S0167-577X\(02\)01377-0](https://doi.org/10.1016/S0167-577X(02)01377-0).
- [216] T.A. Rodrigues, V. Duarte, J.A. Avila, T.G. Santos, R.M. Miranda, J.P. Oliveira, Wire and arc additive manufacturing of HSLA steel: effect of thermal cycles on microstructure and mechanical properties, *Addit. Manuf.* 27 (2019) 440–450, <https://doi.org/10.1016/j.addma.2019.03.029>.
- [217] W. Wu, J. Xue, Z. Zhang, P. Yao, Comparative study of 316L depositions by two welding current processes, *Mater. Manuf. Process.* 34 (13) (2019) 1502–1508, <https://doi.org/10.1080/10426914.2019.1643473>.
- [218] E. Aldalur, F. Veiga, A. Suárez, J. Bilbao, A. Lamikiz, High deposition wire arc additive manufacturing of mild steel: strategies and heat input effect on microstructure and mechanical properties, *J. Manuf. Process.* 58 (2020) 615–626, <https://doi.org/10.1016/j.jmapro.2020.08.060>.
- [219] H. Yi, L. Jia, J. Ding, H. Li, Achieving material diversity in wire arc additive manufacturing: leaping from alloys to composites via wire innovation, *Int. J. Mach. Tools Manuf.* 194 (2024) 104103, <https://doi.org/10.1016/j.ijmachtools.2023.104103>.
- [220] R. Zimermann, E. Mohseni, M. Vasilev, C. Loukas, R.K.W. Vithanage, C. N. Macleod, D. Lines, Y. Javadi, M.P. Espirindio E Silva, S. Fitzpatrick, S. Halavarg, S. McKegney, S.G. Pierce, S. Williams, J. Ding, Collaborative robotic wire + arc additive manufacture and sensor-enabled In-process ultrasonic non-destructive evaluation, *Sensors* 22 (11) (2022), <https://doi.org/10.3390/s22114203>.
- [221] R.P. Ferreira, L.O. Vilarinho, A. Scotti, Development and implementation of a software for wire arc additive manufacturing preprocessing planning: trajectory planning and machine code generation, *Weld. World* 66 (3) (2022) 455–470, <https://doi.org/10.1007/s40194-021-01233-w>.
- [222] M. Jackson, Titanium research developments in the United Kingdom, in: *MATEC Web Conf.*, 2020, p. 321.